https://ntrs.nasa.gov/search.jsp?R=19710024939 2020-03-23T16:09:59+00:00Z

N71-34415

NASA TECHNICAL MEMORANDUM

NASA TM X-67877

NASA TM X-67877

CASE FILE COPY

RELIABILITY TESTING AND DEMONSTRATION AEROSPACE PROBLEMS

by Vincent R. Lalli
Lewis Research Center
Cleveland, Ohio

Lecture Notes for Ninth Annual Reliability Engineering and Management Institute sponsored by the University of Arizona Tucson, Arizona, November 9-13, 1971

RELIABILITY TESTING AND DEMONSTRATION AEROSPACE PROBLEMS

by Vincent R. Lalli
Lewis Research Center
National Aeronautics and Space Administration
Cleveland, Ohio

E-5300-4

INTRODUCTION

The outline shown below describes the types of areospace problems that are explained in these notes. Twenty-three aerospace problems are solved using the various reliability methodologies.

I. APPLICATION OF RELIABILITY METHODS

A. Useful Distribution Functions
1. Derivation of f(t), R(t), λ and λ' functions
2. Estimation using the exponential, normal, Wiebull, gamma and lognormal distributions (Problem 1 to 5)
3. Determination of confidence limits (Problem 6 to 10)
4. Estimation using the Poisson and binomial events (Problem 11, 12)
5. Determination of confidence limits (Problem 13, 14)

B. Sampling
1. Purpose of sampling
2. Choosing a sample (Problem 15)
3. Sample size (Problem 16)

C. Accelerated Life Testing
1. Compressed - time testing (Problem 17)
2. Advanced - stress testing (Problem 18)
3. Optimum life estimate (Problem 19)

I. APPLICATION OF RELIABILITY METHODS

A great deal of work has been done by various researchers to develop probabilistic methods suitable for reliability problems (1, 2, and 3).* Probabilistic methods applying discrete and continuous random variables to aerospace problems is not as well covered in the literature.

In these notes effort will be concentrated on four useful functions: (1) Failure, f(t), (2) Reliability, R(t), (3) Failure Rate, λ, and (4) Hazard Rate, λ'. Since it is usually required to know how well a point estimate has been defined, some consideration will be given to confidence intervals for these functions. The notes also explain methods for planning events at the critical delivery milestone and close with a brief explanation of two reliability case histories.

A. Useful Distribution Functions

The failure function, f(t), which defines failures as a function of time or cycles is very important knowledge obtained from reliability testing. Failure records are kept on a particular piece of hardware to obtain a histogram of failures against time. This histogram is studied to determine which failure distribution fits the existing data best. Once a function for f(t) is obtained reliability analysis can proceed. In many cases time is not available to obtain large quantities of failure density function data. In these cases past experience can be used to determine which failure frequency function best fits a given set of data. Table I lists seven distributions; five continuous and two discrete, showing the time to failure fit for various components. The derivation of the four reliability functions for the seven listed distributions is explained in the next section (4).

---

*Numbers in brackets correspond with referenced documents.

1. Derivation of Q(t), R(t), λ and λ' functions - the unreliability function, Q(t), is the probability that in a random trial, the random variable is not greater than t; hence,

$$Q(t) = \int_0^t f(t)dt$$

When time is our variable, the usual range is 0 to t implying that the process operates for some finite time interval. This integral is used to define the unreliability function when failures are being considered.

The reliability function, R(t), is given by,

$$R(t) = 1 - Q(t)$$

In integral form R(t) is given by,

$$R(t) = -\int_t^\infty f(t)dt$$

Differentiation yields,

$$\frac{dR(t)}{dt} = -\frac{dQ(t)}{dt} = -f(t)$$

The a-posterior probability of failure, p_f, in a given time interval, t_1 to t_2, can be calculated using these equations and is given by,

$$p_f = \frac{1}{R(t_1)}\left[\int_{t_1}^{t_2} f(t)dt\right] = \frac{1}{R(t_1)}\left[\int_{t_1}^{\infty} f(t)dt - \int_{t_2}^{\infty} f(t)dt\right]$$

substituting and simplifing gives,

$$p_f = R(t_1) - \frac{R(t_2)}{R(t_1)}$$

The rate at which failures occur in a time interval is defined as the ratio of the probability of failure in the interval to the interval length. Thus, the equation for failure rate, λ, is given by,

$$\lambda = \frac{R(t_1) - R(t_2)}{(t_2 - t_1)R(t_1)} = \frac{1}{h}\left[1 - \frac{R(t_2)}{R(t_1)}\right]$$

Substituting $t_1 = t$ and $t_2 = t + h$ into this equation gives,

$$\lambda = \frac{R(t) - R(t+h)}{(t + h - t)R(t)} = \frac{R(t) - R(t + h)}{hR(t)}$$

Instantaneous failure rate in reliability literature is in many cases called the hazard rate. Hazard rate, λ', is by definition the limit of the failure rate as $h \to 0$. Using a previous equation and taking the limit of the failure rate as $h \to 0$ gives,

$$\lambda' = \lim_{h \to 0} \frac{R(t) - R(t + h)}{hR(t)}$$

Letting $h = \Delta t$, in this equation gives,

$$\lambda' = \lim_{\Delta t \to 0} -\frac{1}{R(t)}\left[\frac{R(t + \Delta t) - R(t)}{\Delta t}\right]$$

The term in brackets is recognized from the calculus to be the derative of R(t) with respect to time and the negative of this derative is equal to f(t). Substituting these values gives,

$$\lambda' = -\frac{1}{R(t)}\left[\frac{dR(t)}{dt}\right] = \frac{f(t)}{R(t)}$$

As an example consider a jet airplane traveling from Cleveland to Miami. This distance is about 1500 miles and could be covered in about $2\frac{1}{2}$ hours. The average rate of speed would be 1500 miles per 2.5 hours or 600 miles per hour. The instantaneous speed may have varied anywhere

from 0 to 700 miles per hour. The air speed at any given instant could be determined by reading the speed indicator in the cockpit. Replace the distance continuum by failures, failure rate is analogous to average speed, 600 miles per hour in this illustration, and hazard rate is analogous to instantaneous speed, the speed indicator reading in this example.

Figure 1 shows a summary of the useful frequency functions for the failure distributions given in table I. These functions were derived using the defining equations given above. Choose any failure function and verify that R(t), λ and λ' are properly defined by applying the above derived equations. Five aerospace problems using the continuous distributions given in figure 1 are solved in the next section.

2. Estimation using the exponential, normal, weibull, gamma and lognormal distributions - As an example of how to use these equations for an electrical part that experience indicates will follow the exponential distribution, consider Problem 1:

Problem 1

Testing of a particular tantalum capacitor showed that the failure density function was exponentially distributed. For the 100 specimens tested, it was found that $\bar{t}$, the mean-time-between failures, was 1000 hours.

(a) Calculate the hazard rate.

(b) What is the failure rate at 100 hours during the next 10-hour interval?

(c) What are the failure and reliability time functions?

(a) Using the equations given in figure 1 for distribution1; the hazard rate is given by,

$$\lambda' = \frac{1}{t} = \frac{1}{1000 \text{ hours/failure}}$$

or

$$\lambda' = 1 \times 10^{-3} \text{ failures/hours}$$

(b) The failure rate is given by,

$$\lambda = \frac{1}{h}\left(1 - \frac{e^{-t_2/\bar{t}}}{e^{-t_1/\bar{t}}}\right)$$

For this case, the time interval is given by,

$$h = t_2 - t_1 = 110 - 100 = 10 \text{ hours}$$

The necessary reliability functions are given by,

$$e^{-t_2/\bar{t}} = e^{-110/1000} = e^{-0.1} = 0.8958$$

and,

$$e^{-t_1/\bar{t}} = e^{-100/1000} = e^{-0.1} = 0.9048$$

Substituting these values gives,

$$\lambda = \frac{1}{10}\left(1 - \frac{0.8958}{0.9048}\right) = 1\times10^{-3} \frac{\text{failures}}{\text{hours}}$$

This is to be expected for the exponential case as the failure rate is constant with time and always equal to the hazerd rate. (c) The failure and reliability time functions are given by,

$$f(t) = \frac{1}{1000} e^{-t/1000}, \text{ and } R(t) = e^{-t/1000}$$

As an example of how to use the equations given in figure 1 for distribution 2 on mechanical parts subject to wear which follow the normal distribution, consider Problem 2:

Problem 2 (analytical procedure)

A gimbal actuator is being used where friction, mechanical loading and temperature are the principal failure causing stresses. Assume that tests to failure have been conducted for the mechanical parts resulting in the data shown in table II.

(a) Calculate the mean-time-between-failures and standard deviation.

(b) What are the hazard rate at 85.3 K hours and failure rate during the next 10.3 K hour interval?

(c) What are the failure and reliability time functions?

(a) The mean-time-between-failures is given by,

$$\bar{t} = \frac{\sum_{f=1}^{n} t_f}{n}$$

where,

$\bar{t}$ mean-time-between-failures: hr

t_f time-to-failure: hr

n number of observations

Therefore, using the data from table II,

$$\bar{t} = \frac{750 \text{ K}}{10} = 75 \text{ K hours}$$

The unbiased standard deviation, σ, is given by,

$$\sigma = \left[\frac{\sum_{f=1}^{n} t_f^2 - \frac{\left(\sum_{f=1}^{n} t_f \right)^2}{n}}{n - 1} \right]^{1/2}$$

The sum terms required for this calculation are given by,

$$\left(\sum_{f=1}^{n} t_f^2\right) = 5.7213\times10^4 (\text{K hr})^2 \text{ column 3, table II,}$$

and,

$$\left(\sum_{f=1}^{n} t_f\right)^2 = (7.5\times10^2)^2 = 5.625\times10^5 (\text{K hr})^2$$

$$\sigma = \left(\frac{57213 - 56250}{9}\right) = \left(\frac{963}{9}\right)^{1/2} = 10.3 \text{ K hr}$$

(b) The hazard rate, λ', is given by,

$$\lambda' = \frac{\text{normal ordinate at } 85.3 \text{ K hr}}{\text{normal area } 85.3 \text{ K hr to } \infty}$$

Let

$$Y_1 = \text{normal ordinate at } 85.3 \text{ K hr}$$

and Z_1 = standardized normal variable which is given by,

$$Z_1 = \frac{t - t}{\sigma} = \frac{(85.3 - 75.0) \text{ K hr}}{10.3 \text{ K hr}}$$

Existing tables for the normal ordinate values for $Z = +1.0$ gives $Y_1' = 0.242$. The scale constant, K_s, to modify this ordinate value for this problem is given by (5),

$$K_s = \frac{n\theta}{\sigma}$$

where θ = class interval. Substituting values and solving for Y_1 gives,

$$Y_1 = f(t_1) = K_s Y_1' = \frac{10 \times 1 \text{ F}}{10.3 \text{ K hr}} \times 0.242 = 2.35\times10^{-4} \text{ F/hr}$$

It will be noted that the denominator required to calculate λ' is $R(t_1)$; $R(t_1)$ = normal area 85.3 hr to ∞. From existing tables for normal area for $Z_1 = +1.0$ (5), these tables give the area from $-\infty$ to Z_1, so the unreliability $Q(t_1)$ is given by,

$$Q(t_1) = 0.841 \text{ area from } -\infty \text{ to } Z_1$$

Since $Q(t_1) + R(t_1) = 1.000$

then,

$$R(t_1) = 1.000 - 0.841 = 0.159$$

and the hazard rate is given by,

$$\lambda' = \frac{2.35\times10^{-4} \text{ F/hr}}{1.59\times10^{-1}} = 1.47\times10^{-3} \text{ Failures/hr}$$

The failure rate is given by,

$$\lambda = \frac{1}{h}\left[1 - \frac{R(t_2)}{R(t_1)}\right]$$

In this case h is given as 10.3 K hrs. The reliability at 95.6 K hrs is given by,

$$R(t_2) = \text{normal area 95.6 K hr to } \infty$$

Using the same procedure as given above, $R(t_2)$ is given by,

$$R(t_2) = 0.023$$

Substituting values gives,

$$\lambda = \frac{1}{10.3 \text{ K hr}}\left(1 - \frac{0.023}{0.159}\right) = \frac{8.56\times10^{-1}}{1.03\times10^{4}} = 8.31\times10^{-5} \text{ Failures/hr}$$

(c) The constants required to write expressions for f(t) and R(t) are calculated as follows:

$$\frac{1}{\sigma\sqrt{2\pi}} = \frac{1}{1.03\times10^{4} \times 2.52} = 3.87\times10^{-5}$$

$$2\sigma^{2} = 2 \times (1.03\times10^{4})^{2} = 2.12\times10^{8}$$

Using the constants and substituting values gives,

$$f(t) = 3.87\times10^{-5}\, e^{-(t-7.5\times10^{4})^{2}/2.12\times10^{8}}$$

$$R(t) = 3.87\times10^{-5} \int_{t}^{\infty} e^{-(t - 7.5\times10^{4})^{2}/2.12\times10^{8}}\, dt$$

As an example for an electromechanical part which is described by the Weibull distribution consider Problem 3 below:

Problem 3

A lot of 100 stepping motors were tested to see that the reliability functions were for these devices. A power supply furnished electrical pulses to each motor. Instrumentation recorded the number of continuous steps the motors made before it failed to step even though a pulse was provided. All testing was stopped at 1×10^{6} steps. The step failure data are given in table III.

(a) Calculate the frequency functions.

(b) Plot the hazard rate function on log-log paper.

(c) What conclusions can be drawn from this graph?

Since there are 100 motors in this lot, the above data gives percent failure age suitable for plotting on Weibull probability paper. Figure 2 shows a plot of this data. Look at the shape of the data in figure 2. It appears as

though two straight lines are necessary to fit this failure density function. This means that different frequency functions exist at different times. These frequency functions are said to be separated by a partition parameter given by the symbol delta, δ.

From figure 2 the Weibull scale, shape and location parameters can be estimated by following the steps listed below:

(1) Partition parameter estimate (δ).

This estimate can be obtained directly from figure 2. The two straight lines which best fit the given data intersect at point f. Projecting this point down to the abscissa gives a failure age of 10×10^{-3} cycles for the partition parameter, δ.

(2) Location parameter estimate (γ).

γ is used as a straightener for f(t). Since f(t - 0) is already a straight line for both regions, it is clear that $\gamma_1 = \gamma_2 = 0$. In general, several tries at straightening may be required before the yielding a straight line for f(t - γ) is determined.

(3) Shaping parameter estimate (β).

The intercept point a for line b, drawn parallel to line c and passing through point d, where $\ln(t - \gamma) = 1$ is equal to β. Thus $\beta_1 = 0.75$ and $\beta_2 = 1.50$.

(4) Scale parameter estimate (α)

At point e for line c, $\ln \alpha = -\ln \ln 1/1 - Q(t)$, so that $\alpha = e^{-\ln\ln 1/1-Q(t)}$ Therefore,

$$\alpha_1 = e^{2.75} = 15.7$$

$$\alpha_2 = e^{4.6} = 100$$

Using the parameters estimated above and the equations given in figure 1 for Distribution 3, the failure frequency functions can be expressed as listed below.

(a) The partition limits on c are,

$$0 \leq c \leq 10$$

and

$$c > 10$$

The frequency functions are given by,

$$f(c) = \frac{\beta}{\alpha} (c - \gamma)^{\beta-1} e^{-\left[(c-\gamma)^{\beta}/\alpha\right]}$$

substituting values,

$$f_1(c) = \frac{0.75}{15.7} (c)^{0.75-1} e^{-\left(c/15.7\right)^{0.75}}$$

or

$$f_1(c) = 0.047(c)^{-0.25} e^{-(c)^{0.75/15.7}} \quad (0 \leq c \leq 10)$$

Similarily,

$$f_2(c) = 0.015(c)^{+0.5} e^{-(c)^{1.50/100}} \quad (c > 10)$$

The reliability functions are given by,

$$R(c) = e^{-(c-\gamma)^{\beta/\alpha}}$$

therefore, substituting values,

$$R_1(t) = e^{-(c)^{0.75/15.7}} \quad (0 \leq c \leq 10)$$

and

$$R_2(t) = e^{-(c)^{1.50/100}} \quad (c > 10)$$

The failure rate functions are given by,

$$\lambda = \frac{1}{h}\left[1 - \frac{e^{-(c_2-\gamma_1)^{\beta_1/\alpha_1}}}{e^{-(c_1-\gamma_1)^{\beta_1/\alpha_1}}}\right]$$

therefore, substituting values,

$$\lambda_1 = \frac{1}{h}\left[1 - \frac{e^{-(c_2)^{0.75/100}}}{e^{-(c_1)^{0.75/100}}}\right](0 \leq c \leq 10)$$

and

$$\lambda_2 = \frac{1}{h}\left[1 - \frac{e^{-(c_2)^{1.5/100}}}{e^{-(c_1)^{1.5/100}}}\right](c > 10)$$

The hazard rate functions are given by,

$$\lambda' = \frac{\beta}{\alpha}(c - \gamma)^{\beta-1}$$

Therefore, substituting values,

$$\lambda_1' = 0.047\, c^{-0.25}(0 \leq c \leq 10)$$

and

$$\lambda_2' = 0.015\, c^{+0.5}(c > 10)$$

(b) Using 2 cycle log-log paper and the calculation method shown below, the graph of λ' against c can be obtained:

$$\lambda_1' = 0.047\, c^{-0.25}$$

taking logarithms to the base 10,

$$\log \lambda_1' = \log 0.047 + (-0.25)\log c$$

Useful corollary equations are:

$$10^x = y,\ x = \log Y,\ 10^0 = 1 = 10 \text{ and, } \log 0.047 = \log$$

$$4.7\times10^{-2} = \log 4.7 + (-2)\log 10 = \overline{2}.672 \text{ or } 8.672 - 10$$

For c = 1:

$$\log \lambda_1' = \log 0.047 + (-0.25)\log 1$$

$$\lambda_1' = 0.047$$

For c = 10:

$$\log \lambda_1' = \log 0.047 + (0.25)\log 10$$

$$\log \lambda_1' = \overline{2}.672 - 0.25 = \overline{2}.422$$

$$\lambda_1' = 0.0264$$

In a similar manner solving for λ_2' gives the following data points:

c (steps$\times10^{-3}$)	λ' (failures/cycle)
1	0.047
10	.026
10	.015
100	.15

This data is plotted in figure 3.

(c) The graph indicates that hazard rate is decreasing by 0.25 during the first interval and for the second interval is increasing by 0.50 for each logarithmic unit change of c. It appears that step motors, for first misses,

jump from the infant mortality stage into the wear-out stage without any transition period of random failures with a constant failure rate (6).

As an example of combined mechanical and electrical systems which follow the gamma distribution consider problem 4:

Problem 4

Environmental testing of 10 electric rockets with associated power conditioning has resulted in the ordered time-to-failure data given in table IV.

(a) What is the mean-time-between-failures?

(b) Write the Gamma failure and reliability functions.

(c) What is the hazard rate at 5000 hours?

(d) What is the failure rate at 5000 hours during the next 1000 hour interval?

The essential steps for the graphical solution of this problem are given below (7);

(1) Obtain the median ranks for each ordered position see table IV.

(2) Plot on linear graph paper (10 × 10 to the inch) median ranks against failure age covering the range around 80 percent median ranks.

(3) Fit a straight line to the plotted points. For a median rank of 80 read the corresponding failuure age, t_{80}, in hours. Figure 4 gives a t_{80} 7200 hours.

(4) The time-to-failure data is scaled by using the equation given below:

$$\hat{t}_i = \frac{50}{t_{80}} t_i$$

where

$\hat{t}_i$ i^{th} scaled time-to-failure, hr

t_{80} rough estimate of 80 percent failure time, hr

t_i i^{th} time-to-failure, hr

Table IV gives $\hat{t}_i$ for each ordered sample.

(5) Plot on linear graph paper (10 × 10 to the inch) median ranks against scaled time-to-failure, t_i. Figure 5 shows the plotted data points for this problem.

(6) These data points fit the Gamma curves (dashed) well with a (β) estimate of 2.0; hence it appears as though a two-parameter gamma distribution is required with the location parameter (γ) equal to zero. The non-zero location parameter case is covered in the literature (7).

(7) Overlay the linear axis (10 spaces to the inch) of a sheet of 5 cycle semilog paper corresponding to a (β) of 2.0. Plot on this special graph paper, linear scaled rank against time-to-failure given in table IV.

(8) Fit a straight line through the plotted points. Figure 6 shows the Gamma Plot for this data. Two additional straight lines are shown in this figure. Line 1 was obtained by plotting two known points (0.5, 1) and (20, 8) (7). Line 2 has one point at (0.5, 1) with a slope m. If line 1 was coincident with line 2, the β estimate would be sufficiently accurate.

(9) Since the two lines are not coincident, a closer approximation for (β) is obtained by taking a new midpoint coordinate estimate from figure 6 of 6.8. Using existing charts gives (β) = 2.25 which satisfies the slope criteria (7).

(10) For a shape parameter (β) of 2.25 a linear scale rank of 20 percent applies. Entering figure 6 at this percent ordinate, gives a scale parameter (α) of 2400 hours.

With these graphical construction aids the problem solution is readily achieved:

(a) The mean-time-between-failures is given by,

$$\bar{t} = \alpha\beta = 2.4\times10^3 \text{ hours} \times 2.25 = 5.4\times10^3 \text{ hours}$$

(b) The gamma failure and reliability functions are given by,

$$f(t) = \frac{1}{\alpha^{\beta}\Gamma(\beta)} (t - \gamma)^{\beta-1} e^{-(t-\gamma)/\alpha}$$

It has been shown that $\gamma = 0$; the other constants are calculated as follows:

$$\alpha^{\beta} = (2.4\times10^{3})^{2.25}$$

using logarithms, $\log \alpha^{\beta} = 2.25(\log 2.4 + \log 10^{3})$, performing the indicated operations, $\log \alpha^{\beta} = 7.61$; hence, $\alpha^{\beta} = 4.25\times10^{7}$.

The second required constant is $\Gamma(\beta) = \Gamma(2.25)$, using the identity, $\Gamma(x + 1) = X!$, then, $\Gamma(2.25) = \Gamma(1.25 + 1) = 1.25!$, using Sterling's formula, $X! = X^{X}e^{-X}(2\pi X)^{1/2}$, taking logarithms,

$$\log X! = X \log X + (-X)\log e + \left(\frac{1}{2}\right)[\log 2\pi + \log X]$$

$$= \left(X + \frac{1}{2}\right)\log X - 0.434\, x + 0.399$$

$$\log(1.25!) = 1.75 \log 1.25 - 0\ 434\ x\ 1.25 + 0.399$$

$$\log(1.25!) = 0.026$$

Substituting and forming the product, $\alpha^{\beta}\Gamma(\beta) = 4.24\times10^{7}\times1.06 = 4.5\times10^{7}$. Using these constants and substituting values f(t) and R(t) are given by,

$$f(t) = \frac{1}{4.51\times10^{7}}\, t^{1.25}\, e^{-t/2.4\times10^{3}}$$

and

$$R(t) = \frac{1}{4.5\times10^{7}} \int_{t}^{\infty} t^{1.25}\, e^{-t/2.4\times10^{3}}\, dt$$

(c) The hazard rate function at 5000 hours is given by,

$$\lambda' = \frac{f(t_1)}{R(t_1)}$$

here,

$$f(t_1) = \frac{1}{4.51\times10^{7}} (5\times10^{3})^{1.25} e^{\frac{-5\times10^{3}}{2.4\times10^{3}}}$$

performing the indicated operations,

$$f(t_1) = \frac{4.21\times10^{4} \times 1.25\times10^{-1}}{4.5\times10^{7}} = 1.17\times10^{-4}$$

$R(t_1)$ can be obtained either analitically using the above intergral equation or graphically from figure 6. Enter figure 6 at a failure age of 5000 hours. Draw a vertical line to line 3. Project the intersection of Q(t) and 5000 hours over to the linear scale rank (0.605). Using a previous identity,

$$R(t_1) = 1 - 0.605 = 0.395$$

Substituting values gives,

$$\lambda' = \frac{1.17\times10^{-4}}{3.95\times10^{-1}} = 2.71\times10^{-4} \frac{\text{Failures}}{\text{hour}}$$

(d) The failure rate function at 5000 hours during the next 1000 hour interval is given by,

$$\lambda = \frac{1}{t_2 - t_1} \left[1 - \frac{R(t_2)}{R(t_1)} \right]$$

Following the procedure given above and substituting values,

$$R(t_2) = 1 - 0.710 = 0.295$$

and

$$\lambda = \frac{1}{10^3}\left[1 - \frac{0.295}{0.395}\right] = 2.65\times10^{-4}\ \frac{\text{Failures}}{\text{hour}}$$

As an example of mechanical parts under tension stress loading which follow the lognormal distribution consider problem 5 below:

Problem 5

A cable used as guy supports for sail experiments in wind tunnel testing exhibited the time-to-failure performance data given in table V.

(a) Write the failure and reliability functions.

(b) What is the hazard rate at 5715 hours?

(c) What is the failure rate during the next 3000 hours?

(a) The essential steps for solving this problem are given below:

(1) Obtain the median rank for each ordered position see table V.

(2) Plot on lognormal probability graph paper (probability × 2 log cycles median ranks against failure age as shown in figure 7).

(3) If a straight line can be fit to these plotted points, then the time-to-failure function is lognormal.

(4) The mean-time-between-failures is calculated by $t' = \ln(\bar{t})$ where $\bar{t} = 6970$ hours as shown in figure 7 for a median ranks of 50 percent, hence $\bar{t}' = 8.84$.

(5) The standard deviation is given by,

$$\sigma_{t'} = \left[\frac{\ln t_U - \ln t_L}{3}\right]$$

where $t_U = 49\ 500$ hours and $t_L = 1020$ hours as shown in figure 7 for a median and 1-rank of 93.3 percent; hence $\sigma_{t'} = [10.81 - 6.93/3] = 1.28$.

Using these constants the expressions for f(t) and R(t) are written below;

$$f(t) = \frac{3.21\times10^{-1}}{t'} e^{-(t'-8.84)^2/3.28\times10}$$

and

$$R(t) = 3.21\times10^{-1} \int_{\ln(t)}^{\infty} e^{-(t'-8.84)^2/3.28\times10} dt$$

(b) The lognormal ordinate required for λ' can be calculated using the standarized normal variable table as in problem 2. The lognormal standardized variable is given by,

$$Z_2 = \frac{t' - t'}{\sigma_{t'}} = \frac{8.66 - 8.84}{1.28} = -0.143$$

From existing tables,

$$Y_2' = 0.395$$

and

$$Y_2 = \frac{NY_2'}{\sigma_{t'}} = \frac{10 \times 0.395}{1.28} = 3.09$$

Substituting values gives

$$f(t') = \frac{Y_2}{t} = \frac{3.09}{5.715\times10^3} 5.40\times10^{-4} \frac{\text{Failures}}{\text{hour}}$$

The lognormal area from t' to infinity can be obtained directly from figure 7 using the 1-rank scale. Enter the time-to-failure (ttf) ordinate at 5715 hours; project over to the lognormal life function $Q(t)$ and down to the

1-rank abscissa value of 0.638. Therefore, the hazard rate λ' at 5715 hours is given by,

$$\lambda' = \frac{5.40\times10^{-4}}{6.38\times10^{-1}} = 8.46\times10^{-4}\ \frac{\text{Failures}}{\text{hr}}$$

(c) The failure rate during the next 3000 hours is calculated knowing the $R(t_1) = 0.638$ at ttf = 5715 hours and obtaining $R(t_2) = 0.437$ from figure 7 at ttf = 8715 hours. Therefore, the failure rate is given by,

$$\lambda = \frac{1}{3\times10^{3}}\left(1 - \frac{0.437}{0.638}\right) = 1.05\times10^{-4}\ \frac{\text{Failures}}{\text{hr}}$$

(3) Determination of confidence limits - In sections I.A.1 to I.A.3 statistical estimates of various parameters have been made. Now it is of concern to determine methods for defining the confidence one can place in some of these estimates. In sample problem 1 tantalum capacitors having a one-parameter exponential distribution were studied. For an exponentially distributed population, it has been shown that additional estimates follow the chi-square distribution. As an example of how to determine confidence limits for an exponentially distributed estimate consider problem 6.

Problem 6

One hundred tantalum capacitors were tested for 15 000 hours during which time 15 parts failed. (a) What is the mean-time-between failures? (b) What are the upper and lower confidence limits at 98 percent confidence level?

(a) The mean-time-between failures is given by,

$$\bar{t} = \frac{T}{r} = \frac{15\ 000\ \text{hrs}}{15f} = 1\times10^{3}\ \frac{\text{hours}}{\text{failure}}$$

(b) The upper and lower confidence limits at the 98 percent confidence level are given by,

$$U = \left[\frac{2r}{\chi^2_{[1-(\alpha/2)];2r}} \right] \bar{t}$$

and

$$L = \left(\frac{2r}{\chi^2_{(\alpha/2);2r}} \right) \bar{t}$$

where,

U	upper confidence limit, hr
L	lower confidence limit, hr
T	total observed operating time, hr
χ^2	percentage points of chi-squared distribution
r	the number of failures
$1 - \alpha/2, \alpha/2$	probabilities that t will be in the calculated interval

For a 98 percent confidence level required by this problem,

$$\frac{\alpha}{2} = 0.01, \; 1 = \frac{\alpha}{2} = 0.99, \text{ and } 2r = 30$$

Therefore, the chi-squared distribution values are given by (available from many existing tables),

$$\chi^2_{0.01;30} = 50.9$$

$$\chi^2_{0.99;30} = 14.9$$

Substituting values gives,

$$U = \frac{30 \times 1000}{14.9} = 2013 \text{ hr}$$

and

$$L = \frac{30 \times 1000}{50.9} = 589 \text{ hr}$$

Thus, it is known with 98 percent confidence that the limits of the the time $\bar{t}$ lie between 590 and 2010 hours.

Determining the percentage values for the chi-squared distribution for values of r greater than 30 may also be useful. It has been shown that when

$$r \geq 30, \text{ then } \sqrt{2\chi^2} = \sqrt{2r - 1} \pm Z$$

where Z = area under the normal curve at the specified confidence level. Problem 7 illustrates how this equation is used for confidence interval calculations.

Problem 7

The tantalum capacitors of Problem 6 have been operated for 5000 more hours; five additional units have failed. What are the confidence limits on $\bar{t}$ at the 98 percent confidence level for this additional testing?

For the area under the normal curve from $-\infty$ to Z equal to 0.98, 0.02, existing area tables give Z equal to ± 2.06 and,

$$r = 15 + 5 = 20 \text{ total failures, with } 2r = 40$$

Substituting values gives,

$$\sqrt{2\chi^2} = \sqrt{2 \times (40) - 1} \pm 2.06$$

$$\chi^2_{0.01;40} = 59.7, \quad \chi^2_{0.99;40} = 23.4$$

Hence,

$$U = \frac{40 \times 10^3}{23.4} = 1709 \text{ hr}$$

$$L = \frac{40 \times 10^3}{59.7} = 670 \text{ hr}$$

Thus, it can be said, with 98 percent confidence that t lies between 670 and 1710 hours; as the test time increases, the estimated parameters confidence interval decreases.

In sample problem 2 gimbal actuators which exhibited time-to-failure data that was normally distributed were analyzed. For a normally distributed population, additional mean estimates will also be normal. As an example of how to determine confidence intervals for normal estimates consider problem 8.

Problem 8

Twenty-five (25) gimbal actuators have been tested to failure. The mean-time-between failures has been calculated to be 75K hours with a standard deviation of 10.3K hours (see problem 2). (a) What are the upper and lower confidence limits at a 90 percent confidence level?

(a) The upper and lower confidence limits are given by,

$$U = \bar{t} + K_{\alpha/2} \frac{\sigma}{\sqrt{n}}$$

$$L = \bar{t} - K_{\alpha/2} \frac{\sigma}{\sqrt{n}}$$

where,

$\bar{t}$ mean-time-between failures, hr

$K_{\alpha/2}$ standarized normal variable

σ unbiased standard deviation

n number of samples

$1 - \alpha$ probability that $\bar{t}$ will be in the calculated interval

For this problem,

$$1 - \alpha = 0.90, \quad \alpha = 0.10, \quad \frac{\alpha}{2} = 0.05$$

and

$K_{\alpha/2}$ from existing tables is $K_{\alpha/2} = 1.64$

Substituting values gives,

$$U = 75K + \frac{1.64 \times 10.3K}{\sqrt{25}} = 78.4 \text{ K hr}$$

and

$$L = 75K - \frac{1.64 \times 10.3K}{\sqrt{25}} = 71.6 \text{ K hr}$$

This means that 90 percent of the time the mean-time-between-failures estimate, $\bar{t}$, for 25 gimbal actuaters, rather than the original, 10 will be between 71 600 and 78 400 hours. It is important to note that the sample size has been increased to use the above technique. This reflects a usual aerospace pressure, learn as much as possible with the least amount of testing. Try to keep $n \geq 25$ for estimating normal parameters with the above technique.

If the sample size, $n < 25$ then use should be made of the Student's t Distribution (8). To determine the effects of reducing sample size on confidence intervals, reworking problem 6 for the smaller sample size of 10, using the Student t Distribution. The upper and lower confidence limits are given by,

$$U = \bar{t} + t_{\alpha/2} \frac{s}{\sqrt{n}}$$

and

$$L = \bar{t} - t_{\alpha/2} \frac{s}{\sqrt{n}}$$

where

$t_{\alpha/2}$ student t variable

s standard deviation

For this problem, $r = n - 1 = 9$, $\alpha = 0.10$ and $t_{\alpha/2}$ from existing tables is $t_{\alpha/2} = 1.83$. The standard deviation is given by

$$s = \left(\frac{57213 - 56250}{10}\right)^{1/2} = 9.82 \text{ K}$$

Substituting values gives,

$$U = 75\text{K} + \frac{1.83 \times 9.82 \text{ K}}{\sqrt{10}} = 80.7 \text{ K hr}$$

and

$$L = 75\text{K} - \frac{1.83 \times 9.82 \text{ K}}{\sqrt{10}} = 69.3 \text{ K hr}$$

Comparing this time interval with that calculated for a sample size of 25 shows that the smaller sample size gives a larger interval of uncertainty.

In sample problem 3 stepping motors which exhibited time-to-failure data that was Weibull distributed were studied. As a graphical example of how to determine confidence intervals for a Weibull distributed estimate consider problem 9.

Problem 9

Another group of stepping motors has been step tested as previously explained in sample problem 3. The Weibull plot of percent failures for a given failure-age is the same as given in figure 2. During this testing, however, only 8 failures have occurred. What is the 90 percent confidence band on the reliability estimate at 4000 cycles?

The data needed for graphical construction of the confidence lines on the Weibull plot is given in table III. The steps necessary to construct the confidence lines in figure 2 are as follows (9):

(1) Enter the percent failure axis with the first 5 percent rank value hitting Q(t); failure 2, 5 percent rank 3.68.

(2) Draw a horizontal line which intersects Q(t) at point 1.

(3) Draw a vertical line to cross the corresponding median rank; failure 2, median rank 16.23.

(4) Draw a horizontal line at the median rank, 16.23, for failure 2. The intersection point of the line for step 3 with this line is one point on the 95 percent confidence line.

(5) Repeat steps 1 to 4 until the desired cycle life is covered, 4000 cycles in this case.

(6) The 5 percent confidence line is obtained in a similar manner. Enter the percent failure axis with the 95 percent failure rank, 25.89 for failure 1.

(7) Draw a horizontal line which intersects Q(t) at point 3.

(8) Draw a vertical line to cross the corresponding median rank; failure 1, median rank 6.70.

(9) Draw a horizontal line at the median rank, 6.70, for failure 1. The intersection point of these two lines is one point on the 5 percent confidence line.

(10) Repeat steps 6 to 9 until the desired cycle life is covered.

At 4000 cycles a 90 percent confidence interval for Q(t) is from figure 2; 1.2 percent, 37.5 percent. Hence, a 90 percent confidence interval for R(t) at 4000 cycles is 0.998 to 0.625.

In sample problem 5 guy supports which exhibited time-to-failure data that was lognormally distributed were analyzed. As a final graphical example of how to determine confidence intervals for a lognormal distributed estimate consider problem 10.

Problem 10

It has been shown that the guy supports of problem 5 exhibited a reliability of 0.638 at a ttf of 5715 hours. Consider now the procedure for determining the confidence band on this lognormal estimate. The data needed for the graphical construction of the 90 percent confidence lines on the lognormal graph of figure 7 is also given in table V. The steps necessary to graphically construct the confidence lines in figure 7 are as follows:

(1) Enter the ranks axis with the first 5 percent rank value hitting Q(t) the lognormal life function shown in figure 7; ordered sample number 3, 5 percent rank 8.7.

(2) Draw a vertical line to intersect Q(t) at point 1 as shown in figure 7.

(3) Draw a horizontal line to cross the corresponding median rank; ordered sample number 3, median rank 25.9.

(4) The intersection point (point 2 in fig. 7) of step 3 and the median rank line is one point on the 95 percent confidence line.

(5) Repeat steps 1 to 4 until the desired time-to-failure is covered, 5715 hours in this case.

(6) The 5 percent confidence line is obtained in a similar manner. Enter the ranks axis with the 95 percent failure rank, 25.9 for ordered sample number 1.

(7) Draw a vertical line which intersects Q(t) at point 3.

(8) Draw a horizontal line to cross the corresponding median rank; ordered sample number 1, median rank 6.7.

(9) The intersection point (point 4 in fig. 7) of these two lines is one point on the 5 percent confidence line.

(10) Repeat steps 6 to 9 until the desired time-to-failure is covered.

At 5715 hours the 90 percent confidence interval for Q(t) is from figure 7: 19.7 percent, 69.4 percent. Hence, a 90 percent confidence interval for R(t) at 5715 hours is 0.803 to 0.306. Incidentally, this graphical procedure for finding confidence intervals is completely general and can be used on other types of life test diagrams.

4. Estimation using the Poisson and binomial events

The binomial and Poisson distributions are discrete functions of the number of failures, N_f, which occur rather than time, t.

The Poisson Distribution given in figure 1 as distribution 6 is a discrete function of the number of failures. When this distribution applies it is of interest to determine the probabilities associated with a specified number of failures in the continuum of time. As an example for a complex electrical component which follows the Poisson Distribution consider problem 11.

Problem 11

Ten space power speed controllers were tested during the Sunflower development program. The time-to-failure test data is given in table VI.

(a) Write the Poisson failure density and reliability functions.

(b) What is the probability of five failures in 10 000 hours?

(c) What is the probability that 6, 7, 8, 9, or 10 failures will occur or the reliability from the 5th failure?

(a) Reducing the data given in table VI, the mean-time-between failures is given by,

$$\bar{t} = \frac{\sum_{i=1}^{10} t_i}{N_f} = \frac{8.586\times10^4}{10} = 8.59\times10^3 \ \frac{\text{hr}}{\text{failures}}$$

hence, the Poisson failure density function is given by,

$$f(N_f) = \frac{(t/8.59\times10^3)^{N_f}}{N_f!} e^{-t/8.59\times10^3}$$

The reliability function is given by,

$$R(N_f) = \sum_{j=1}^{10} \frac{(t/8.59\times10^3)^j}{j!} e^{-t/8.59\times10^3}$$

(b) To calculate, the probability of five failures f(5) in 10 000 hours, use if made of the ratio $(t/\bar{t})$ which is given by,

$$\frac{t}{\bar{t}} = \frac{1.0\times10^4}{8.56\times10^3} = 1.16$$

The probability of five failures in 10 000 hours is given by,

$$f(5) = \frac{(1.16)^5 e^{-1.16}}{5!} = \frac{2.09 \times 0.314}{1.2\times10^2} = 5.47\times10^{-3}$$

One easy method to calculate the term $(1.16)^5$ is as follows:

$$\log(1.16)^5 = 5 \log 1.16 = 5(0.148) = 0.740$$

$$(1.16)^5 = 2.09$$

(c) The reliability from the 5th to the 10th failure is the sum of the remaining terms in the Poisson expansion. The Poisson expansion in sum form is given by,

$$R(N_f) = \sum_{j=6}^{10} \frac{0.314(1.16)^j}{j!}$$

Calculating each term and summing gives,

$$R(6) = 0.0013$$

The binomial distribution is given in figure 1 as distribution 6. Considerable work has been done to develop the techniques suitable for use of this powerful tool (3, 5, and 10). As an example consider a pyrotechnic part described in sample Problem 12.

Problem 12

A suspicious lot of explosive bolts is estimated to be 15 percent defective due to improper loading density observed in neutron radiography.

(a) Calculate the probability of one defective unit appearing in a flight quantity of four.

(b) Plot the resulting histogram.

(c) What is the reliability from the first defect?

Not much failure density data is available, however, past experience with pyrotechnic devices has shown that the binomial distribution applies. From the given data,

q per unit number of effectives = 0.85

p per unit unit of defectives = 0.15

n sample size = 4

N_f possible number of failures = 0, 1, 2, 3, 4

The frequency functions corresponding to these constants are given by,

$$f(N_f) = \frac{4!}{(4 - N_f)!\ N_f!}\ p^{N_f} q^{4-N_f}$$

and

$$R(N_f) = \sum_{j=N_f}^{4} \frac{4!}{(4 - j)!\ j!}\ p^j q^{n-j}$$

One simple method to obtain the binomial expansion coefficients is to make use of Pascal's triangle. Pascal found that there was symmetry to the coefficient development and explained it as shown in table VII. Column 1 gives the sample size, n. Column 2 gives the possible number of failures. Column 3 gives the binomial expansion coefficients. Pascal's triangle (dashed) is shown in column 3, rows 3 and 4. The lower number in the dashed triangle are obtained by adding the two upper numbers to get that number; that is, refer to dashed insertion, two upper 3's summed equal 6, the lower number.

Using these constants and expanding, $f(N_f)$ is given by,

$$f(N_f) = q^4 + 4q^3p + 6q^2p^2 + 4qp^3 + p^4$$

The probability of one defective unit appearing in the flight quantity of 4 is given by the second term in the expansion; hence,

$$4q^3p = 4(0.85)^3(0.15) = 0.37$$

The resulting histogram for this distribution is shown in figure 8. The probability that 2, 3, or 4 defects will occur as the reliability from the first defect is the sum of the remaining terms in the binomial expansion. This probability can be calculated using the equation for $R(N_f)$. However,

it is simpler ot use the histogram graph and sum the probabilities over N_f from 2 to 4; hence,

$$R(2) = 0.096 + 0.011 + 0.0011 = 0.108$$

These explosive bolts in their present form are not suitable for use on any spacecraft as the probability of zero defects is only 0.522 much below the usually desired 0.999 for pyrotechnic spacecraft devices.

5. Determination of confidence limits

When an estimate is made using discrete distributions, it is expected that additional estimates of the same parameter will be close to the original estimate. It is desirable to be able to determine upper and lower confidence limits at some stated confidence level for discrete distribution estimates just as is done for continuous functions of time. The analytical procedure for determining these intervals is simplified by using specially prepared tables and graphs. Useful tables for the binomial distribution are given in the literature (5, 10, 11, and 12)

As an example of how confidence intervals can be obtained for Poisson estimates consider problem 13.

Problem 13

The Poisson estimate of reliability from the 5th to the 10th failure for speed controllers was found to be 0.0013 in a previous problem. What are the upper and lower confidence limits on this estimate at a 95 percent confidence level?

The variation in $\bar{t}$ can be found by using figure 9 (12). Enter figure 9 on the 5 percent α line at the left hand end of the 5 interval, here $T/\bar{t}_1 = 10.5$; then, $\bar{t}_1 = 10\,\bar{t}/T/\bar{t}_1 = 8.57\times10^4/10.5 = \breve{8}160$ hours. Using the left hand end of the 4 interval $T/\bar{t}_2 = 9.25$; then $t_2 = 8.57\times10^4/9.25 = \breve{9}530$ hours.

One simple method to find Q(5) is to use figure 10 (5). The $t/\bar{t}$ ratios of interest are 1.22, 1.16, and 1.05, respectively. For these ratios with $N_f = 5$, the values of Q(5) from figure 10 are 0.997, 0.9987, and 0.99992, respectively. Since the sum of the last five terms is desired, R(5) is 0.003, 0.0013, and 0.0008, respectively.

This means that the probability of the 5th to the 10th failure of a speed control occurring is in the interval from 0.0008 to 0.003 at a confidence level of 95 percent.

As an example of how confidence intervals can be obtained for binomial estimates consider problem 14.

Problem 14

The probability of one defective unit appearing in a flight quantity of four explosive bolts has been calculated to be 0.37. What are the upper and lower confidence limits on this estimate at a 90 percent confidence level?

If the sample size is n, the number of defectives is r and the confidence level is γ, this problem has the following constraints: n = 4, r = 1 and γ = 90 percent. Using these constraints, the upper U and lower L confidence limits can be obtained directly from existing tables (10).

U = 0.680 and L = 0.026

This means that with a 90 percent confidence the probability of one defective bolt appearing in a flight quantity of four is in the interval from 0.026 to 0.680.

B. Sampling

(1) Purpose of sampling - Sampling is a statistical method used when it is not practical to study the whole population. There are usually five basic reasons why sampling is necessary:

(a) Economy - It usually costs less money to study a sample of an item than the whole population.

(b) Timeliness - A sample can be studied in less time than the whole population giving prompt results.

(c) Destructive nature of a test - Some tests require that the end item must be used up to demonstrate performance leaving nothing to use.

(d) Accuracy - A sample survey accomplished by well trained researchers usually will result in accurate and valid decisions.

(e) Infinite population - In many analytical studies an infinite population is available. If any information is to be used for decision making, it must be based on a sample.

(2) Choosing a sample - It is very important to use good judgement in selecting a sample. It has been shown that subjective methods of picking samples frequently results in bias (13). Bias is an expression, either conscious or subconscious, of the selector's preferences. Bias can be held to a minimum by using a nonsubjective method which has been developed just for this purpose. Several nonsubjective sampling procedures are described below:

(a) Random sampling - Each item in the population shall have an equal and independent chance of being selected as a sample. A random digits table, see figure 11, has been developed to facilitate drawing of random samples. This table has been constructed to make the ten digits from 0 to 9 equally likely to appear at any location in the table. Adjacent columns of numbers can be combined to get various sized random numbers.

(b) Stratified sampling - Similar items in a population shall be grouped or stratified and a random sample selected from each group.

(c) Cluster sampling - Items in a population shall be partitioned into groups of clusters and a random sample selected from each cluster.

(d) Double sampling - A random sample shall be selected; depending on what is learned, some action is taken or a second sample is drawn. After the second random sample is drawn action is taken on the basis of data obtained from the combination of both samples.

(e) Sequential sampling - Random samples shall be selected and studied one at a time. A decision on whether to take action or continue sampling shall be made after each observation based on all data available at that selection.

As an example of when to use various sampling methods consider sample problem 15.

Problem 15

Describe how a sample should be selected for the three cases given below:

(a) Invoices numbered from 6721 to 8966 consecutively.

A random sampling procedure could be used in this case based on the four digit table given in figure 11. Using the given invoice numbers, start at the top of the left column and proceed down each column selecting random digits until the desired sample size is obtained. Disregard numbers outside the range of interest.

(b) Printed circuit assemblies to compare the effectiveness of different soldering methods.

If boards are all of the same type a cluster sampling procedure could be used here. Group the boards by soldering methods; select x joints from each cluster to compare the effectiveness of different soldering methods.

(c) Residual gases in a vacuum vessel to determine the partial pressure of gases at various tank locations.

A stratified sampling procedure could be used in this case. Stratify the tank in the vicinity of existing feedthrus into x sections; an appropriate mass run could be taken from each section at various ionizer distances from the tank walls. Analysis would tell how the partial pressures varied with ionizer depth at the feedthru locations.

(3) Sample size - A completely general equation for determining sample size, n, is given by,

$$Q(t) = 1 - R(t_r) = \frac{N_f}{n}$$

where

N_f the desired number of time-to-failure points

n sample size

t_r truncation test time

This equation can be used with any of the reliability functions given in figure 1.

As an example of how these equations can be applied to electrical parts which follow the exponential distribution consider problem 16 which was derived from previous problem 1.

Problem 16

Tantalum capacitors with a failure rate of 1×10^{-3} failures/hour are to be tested to failure. In a 1000 hour test what sample size should be used to get 25 time-to-failure data points?

The truncated exponential reliability function is given by,

$$R(t_r) = e^{-t_r/1000} = 0.37$$

Solving the general sample size equation for n and substituting values gives,

$$n = \frac{N_f}{1 - R(t_r)} = \frac{25}{0.63} = 39.6$$

Rounding of to the nearest whole unit gives n = 40 pieces. This means that 40 capacitors tested for 1000 hours should give 25 time-to-failure data points.

C. Accelerated Life Testing

Life testing to define the time duration during which a device performs satisfactorily is a very important measurement in reliability testing because it is a measure of the reliability of a device. The life a device will exhibit is very much dependent on the stresses it is subjected to. The same devices in field application are frequently subjected to different stresses at varying times. It should be recognized then that life testing involves the following environmental factors:

(a) The use stresses may influence the device's life and failure rate functions.

(b) The field stresses could be multidimensional.

(c) In the multidimensional stress space there is an interdependence among the stress' effects.

(d) Most devices operate over a range in a multidimensional stress space which accounts for some variance in life performance.

Testing objects to failure under multidimensional stress conditions is usually not practical. Even if it was, if the system has been properly designed, the waiting time to failure would be quite long, and therefore, unrealistic. Previously it has been shown that time-to-failure data is very important to reliability testing and now it appears difficult to obtain. These are some of the reasons why many are turning to accelerated life testing.

(1) Compressed-time testing - If a device is expected to operate once in a given time period on a repeated cycle, life testing of this device may by accelerated by reducing the operating time cycle. The multidimensional

stress condition need not be changed. The stresses are being applied at a faster rate to accelerate device deterioration. Care should be taken not to accelerate the repetition rate beyond conditions which allow the device to operate in accordance with specifications. Such conditions would move the device into a multidimensional stress region that does not exist in field conditions and would yield biased information. As an example of compressed-time testing consider problem 17.

Problem 17

The stepping motor in previous sample problem 3 was being pulsed for life testing. How could this life test be accelerated?

The power supply which was providing the stepping pulses may have been stepping at the rate of one pulse per 10 seconds resulting in a test time of 10^7 seconds. These motors had a frequency response allowing for 10 pulses per second. Increasing the pulse stepping rate up to the frequency response limit yields comparable time-to-failure data in 10^5 seconds; a savings in time of two orders of magnitude.

(2) Advanced-stress testing - If a device is expected to operate in a defined multidimensional stress region, life testing of this device may be accelerated by changing the multidimensional stress boundary. Usually the changes will be toward increased stresses as this tends to reduce time waited to failure. There are two basic reasons why advanced stress testing is used:

(a) To save time

(b) To see how a device performs under these stress conditions

Care should be exercised in changing stress boundaries to be sure that unrealistic conditions leading to wrong conclusions are not imposed on the device. A thorough study of the failure mechanisms should be made to ensure that proposed changes will not introduce new mechanisms which are not normally encountered. If an item has a certain failure density distri-

bution in the rated multidimensional stress region, changing the stress boundaries should not change the failure density distribution. Table VIII lists some guidelines for planning advanced-stress tests.

As an example of advanced-stress testing consider problem 18.

Problem 18

A power conditioning supply is being life tested at nominal conditions with an associated electric rocket. The nominal electrical, thermal, vibration, shock and vacuum stresses resulted in fairly long waiting periods to failure. Changing the multidimensional stress conditions by a 1.25 to 2 factor, which is usually done during development testing, tends to identify design deficiencies with shorter waiting periods without affecting the failure mechanism.

(3) Optimum life estimate - One remaining calculation for nonreplacement failure or time truncated life test is the optimum estimate of mean-time-between-failures, $\bar{t}$. It has been shown that $\bar{t}$ given by the time sum divided by the number of failures should be modified by a censorship and a truncation time factor. The censorship factor, K, is caused by wearout failures, operator error, manufacturing errors and things like these. The correction equation for $\bar{t}$ is given by (3),

$$\bar{t} = \frac{\sum_{i=1}^{N_f} t_i + (n - N_f)t_r}{N_f - K}$$

where

N_f number of failures

K censorship failures

As an example consider problem 19.

Problem 19

The tantalum capacitors tested in problem 1 could have been stopped when 10 capacitors (580 piece part-hours) out of 100 had failed at a testing time of 100 hours. What is the optimistic value for $\bar{t}$?

Inspection of the ten failed capacitors showed that two units failed due to manufacturing errors. Under these conditions, $N_f = 10$ failures, $K = 2$ failures, $n = 100$ capacitors, $t_r = 100$ hours and the sum of $t_i = 580$ hours. Substituting values into the $\bar{t}$ correction equation gives,

$$t = \frac{580 + (100 - 10)100}{10 - 2} = 1197 \text{ hours}$$

This is an optimistic estimate for mean-time-between-failures but it certainly is fair and reasonable to make these types of corrections.

D. Accept Reject Decisions With Sequential Testing

A critical milestone occurs in product manufacturing at delivery time. An ethical producer is concerned about shipping a product lot which does not meet specifications. The consumer is concerned about spending money to purchase a product which does not meet the specifications. A test method which permits each to have an opportunity to obtain data for decision making is required.

1. Sequential testing constraints

If (α) is the producer's rask and (β) is the consumer's risk, two delivery time constants valid for small risks have been defined, and are given as,

$$A = \frac{1 - \beta}{\alpha}$$

$$B = \frac{\beta}{1 - \alpha}$$

Let (P_1) be the probability that N_f failures will occur in time t for a specified minimum acceptable $\bar{t}_1$, and (P_o) be the probability that N_f failures will occur in time t for an arbitrarily chosen upper value $\bar{t}_o$.

Using these four constants, test rules have been defined for each condition (3 and 7),

(a) Accept if: $\frac{P_1}{P_o} \leq B$

(b) Reject if: $\frac{P_1}{P_o} \geq A$

(c) Continue testing if: $B < \frac{P_1}{P_o} < A$

2. Exponential parameter decision making

As an example of how these testing constraints can be implemented for the exponential distribution, consider sample problem 20.

Problem 20

A purchased quantity of 100 000 tantalum capacitors has been received. Negotiations prior to placement of the order had established that $\alpha = \beta = 0.1$, $\bar{t}_1 = 1000$ hours, $\bar{t}_o = 2000$ hours and that the sequential reliability test should be truncated in 48 hours.
(a) Calculate A and B; (b) Write the expressions for P_o and P_1; (c) How many units should be placed on test? (d) Plot a sequential reliability control graph to facilitate decision making at each failure time.

(a) The delivery time constants are obtained by substituting values into the defining equations,

$$A = \frac{1 - 0.1}{0.1} = 9$$

$$B = \frac{0.1}{1 - 0.1} = 0.111$$

(b) Using distribution 7 from figure 1 and substituting values, $P_o(N_f)$ and $P_1(N_f)$ are given by,

$$P_o(N_f) = \left(\frac{t}{2000}\right)^{N_f} \frac{e^{-t/2000}}{N_f!}$$

$$P_1(N_f) = \left(\frac{t}{1000}\right)^{N_f} \frac{e^{-t/1000}}{N_f!}$$

(c) Delivery constant B defines the acceptance criteria for P_1/P_o. Using this constraint and substituting for P_1 and P_o gives,

$$B = \frac{P_1(N_f)}{P_o(N_f)} = 2^{N_f} e^{-t/2000}$$

The minimum number of no failure unit - hours of testing time $T(o)_{min}$ is given by,

$$0.111 = (2)^o \, e^{-T(o)_{min}/2000}$$

Solving for $T(o)_{min}$

$$T(o)_{min} = 2.20 \times 2000 = 4400 \text{ unit-hours}$$

The minimum number of capacitors to be life tested for 48 hours is given by,

$$n_{min} = \frac{4400 \text{ unit-hours}}{48 \text{ hours}} = 91.7$$

To insure good results, choose a sample size, n, about twice n_{min}, for this problem use n = 200 units. The required minimum testing time for 200 units is given by,

$$t(o)_{min} = \frac{4400 \text{ unit-hours}}{200 \text{ unit}} = 22.0 \text{ hours}$$

The test can be stopped and an accept/reject decision made at T_r; T_r is given

$$T_r = 48 \text{ hours} \times 200 \text{ unit} = 9.6\times10^3 \text{ unit-hours}$$

(d) The tantalum capacitors reliability chart is constructed using five points in the (N_f, t) plane; three of these points have already been calculated and are given by,

$$T(o)_{min} = 4.4\times10^3, \quad N_f = 0$$

$$T_r = 9.6\times10^3, \quad N_f = 0$$

$$t = 0, \quad N_f = 0$$

The remaining two points are calculated using the test inequality given by,

$$B < p(N_f) < A$$

In general terms the ratio $p(N_f)$ is given by,

$$(N_f) = \left(\frac{t_o}{t_1}\right)^{N_f} e^{-(1/t_1 - 1/t_o)t}$$

Taking natural logarithms of the inequality and substituting gives,

$$\ln B < N_f \ln\left(\frac{\bar{t}_o}{\bar{t}_1}\right) - \left(\frac{1}{\bar{t}_1} - \frac{1}{\bar{t}_o}\right)t < \ln A$$

adding $(1/\bar{t}_1 - 1/\bar{t}_o)t$ to each term gives,

$$\ln B + \left(\frac{1}{\bar{t}_1} - \frac{1}{\bar{t}_o}\right)t < N_f \ln\left(\frac{\bar{t}_o}{\bar{t}_1}\right) < \ln A + \left(\frac{1}{\bar{t}_1} - \frac{1}{\bar{t}_o}\right)t$$

Dividing all terms by $\ln(t_o/t_1)$ gives,

$$\frac{\ln B}{\ln\left(\frac{\bar{t}_o}{\bar{t}_1}\right)} + \left[\frac{\frac{1}{\bar{t}_1} - \frac{1}{\bar{t}_o}}{\ln\left(\frac{\bar{t}_o}{\bar{t}_1}\right)}\right]t < N_f < \frac{\ln A}{\ln\left(\frac{\bar{t}_o}{\bar{t}_1}\right)} + \left[\frac{\frac{1}{\bar{t}_1} - \frac{1}{\bar{t}_o}}{\ln\left(\frac{\bar{t}_o}{\bar{t}_1}\right)}\right]t$$

The inequality is now in the form given by

$$a + bt < N_f < c + bt$$

The constants a and c for this problem for zero failures are given by,

$$a = \frac{\ln B}{\ln\left(\frac{\bar{t}_o}{\bar{t}_1}\right)} = \frac{-2.20}{0.693} = -3.18, \quad N_f = 0$$

$$c = \frac{\ln A}{\ln\left(\frac{\bar{t}_o}{\bar{t}_1}\right)} = \frac{2.20}{0.693} = 3.18, \quad N_f = 0$$

Since these boundary constraints are straight lines in the form $N_f = bt + (a \text{ or } c)$ the slope b is given by,

$$b = \frac{\left(\frac{1}{\bar{t}_1} - \frac{1}{\bar{t}_o}\right)}{\ln\left(\frac{\bar{t}_o}{\bar{t}_1}\right)} = \frac{5\times10^{-4}}{0.693} = 7.22\times10^{-4}$$

Figure 12 shows the resulting tantalum capacitors reliability chart. The tantalum capacitor acceptance reliability test results in an accept, continue to test, or reject decision depending on the failure performance of the capacitors as a function of unit-hours as zoned in figure 12.

3. Binomial parameters dicision making (problem 21)

For parts which follow the binomial frequency function, the procedure to set up a sequential reliability test is very similar to the Poisson methodology. As the unreliability or number of defectives is given by 1 - R for an effectives of R, then $P_1(N_f)$ is given in binomial form by,

$$P_1(N_f) = (1 - R_1)^{N_f}(R_1)^{n-N_f}$$

where

n	$N_s + N_f$
N_s	number of successful trials
N_f	number of failure trials
N_c	choosen units on test
$R_{o,1}$	choosen reliability values at some time, t, $R_o > R_1$

The ratio of $P_1(N_f)/P_o(N_f)$ is given by,

$$P(N_f) = \frac{\left(1 - R_1\right)^{N_f}\left(R_1\right)^{n-N_f}}{\left(1 - R_o\right)^{N_f}\left(R_o\right)^{n-N_f}}$$

where $1 - R_1$, gives the unreliability or the number of defectives (see fig. 1). Following the same steps as given in sample problem 20, gives the four points in the (N_f, n) plane,

$$N(o)_{min} = \frac{\ln B}{\ln\left(\frac{R_1}{R_o}\right)}, \quad N_f = 0$$

$$N_r = t_r x N_c, \quad N_f = 0$$

$$n = 0, \quad N_f = 0$$

$$a = \frac{\ln B}{\ln \frac{R_o(1 - R_1)}{R_1(1 - R_o)}}, \quad N_f = 0$$

$$c = \frac{\ln A}{\ln \frac{R_o(1 - R_1)}{R_1(1 - R_o)}}, \quad N_f = 0$$

The slope b is given by,

$$b = \frac{\ln\left(\frac{R_o}{R_1}\right)}{\ln \frac{R_o(1 - R_1)}{R_1(1 - R_o)}}$$

The inequality equation for these conditions is given by

$$a + bn < N_f < c + bn$$

Accept/reject decisions at delivery milestones when based on reliability sequential testing methods provides a rigerous mathematical method to decide whether or not to accept or reject an order of components. The actual reliability value for these components is not known, nor is it wise to consider reliability assessment at this critical milestone. The exhibited mean-time-between-failures can be calculated later using the method explained in Procedure 28.0 of the SERT II Manual (14).

II. RELIABILITY CASE HISTORIES

The Lewis Research Center's reliability engineering programs are designed to require:

(1) Through planning and effective management of the reliability assurance effort.

(2) Definition of the major reliability engineering tasks and their place as an integral part of the design and development process.

(3) Assurance of reliability through a complementary program of reliability engineering and evaluation.

A. SERT II Project (Problem 21)

The second Space Electric Rocket Test (SERT II) Program was conducted by the Lewis Research Center of the National Aeronautics and Space Administration in 1970. The primary purpose of the program was to demonstrate the technology of a light weight, ion thruster and power conditioning

system for long-life space applications. This was partially accomplished by operating the system in space for 5 of the 6 desired months. In order to obtain continuous sunlight for this period, the spacecraft was launched into polar orbit from the Western Test Range in California. Figure 13 depicts the launch trajectory and orbit path. Each thruster system failed by a previous unknown zero G failure mode, errosion bridging. Metal particles following the electric field lines build a bridge from accelerator to screen. Known design changes can eliminate this failure mode for future missions.

A reliability engineering effort was established and maintained to assure that the complete space system, launch vehicle, spacecraft and associated ground support equipment were capable of meeting the SERT II objectives.

The SERT II design concept was strongly influence by the philosophy of maximum utilization of previously space qualified hardware, of system redundancy, and of extensive endurance testing of a complete spacecraft under simulated mission conditions. With few exceptions new design was limited to supporting on-board experiments of secondary mission criticality. For all new designs minimum parts derating factors were employed. For newly designed critical components, a review of such factors as complexity, exposure to transients, redundancy, and the scope and depth of the planned test program were used to determine the need for formal stress analysis. Similar considerations were given to the need for formal failure mode, effect and criticality analysis.

1. Implemented provisions

The nine reliability provisions implemented on the SERT II Project are listed and explained below:

Design review

Formal design reviews conducted by the Project Office did include participation by R&QAO. The R&QAO did provide an independent appraisal of the design

under consideration giving special attention to its reliability preformance. These R&QAO representatives did provide follow-up action on items related to reliability areas of concern.

Projected analyses for newly designed critical systems was developed to determine possible modes of failure and their effect. The primary objective of these analyses was to discover critical failure areas and remove susceptibility to such failures from the system. In the analyses, each potential failure was considered in the light of probability of occurrence and was categorized as to probable effect on mission success of the system to aid in proportioning effort for corrective design action. These analyses were a major consideration in design reviews and also provided an important criterion for test planning.

Reliability modeling

A reliability prediction model was made to show that the system was capable of meeting the specified MTBF goals. Each functional device, input, output, internal and external connection point and boundary was shown in a system block diagram. The model was revised as required by evaluation of the design, design changes, and test data. This model was used as:

(a) A basis for redundancy.

(b) A guide for reliability improvements.

(c) A guide for failure data reporting and analysis.

Parts and materials selection

The R&QAO did support the Project Office in selection, reduction in number of types, specifications, qualification and application review of parts and materials. R&QAO did review nonstandard parts (i.e., parts selected from sources other than preferred parts lists) and recommend their suitability for use on program hardware.

Stress analysis

Newly designed critical components and subsystems were studied analytically and experimentally to determine the electrical, mechanical and thermal stresses to verify that the designs have adequate derating factors for spacecraft use. Steady state and transient stress were measured. Operating magnitude or shutdown were studied to determine worse case conditions.

In cases where the derating factors cannot be achieved, a derating factor nonconformance list was prepared. This list was reviewed by R&QAO and recommendations for corrective action submitted to the Project Manager.

Electrical

Electrical measurements were made on the developmental model in a laboratory environment. This survey measured the voltage, current and power for parts operating at over 50 percent of their rating or dissipating more than 0.5 watts.

Thermal

A preliminary thermal survey was conducted on the developmental models in a laboratory environment. This survey measured the surface or case temperature of each critical or questionable part. A second thermal survey was conducted on the prototype models mounted to demonstrate compliance with flight environmental specifications.

Mechanical

A mechanical survey was conducted on the prototype models mounted to demonstrate proper derating for shock, vibration and acceleration in compliance with flight environmental specifications.

Failure, reporting, analysis and corrective action

An integrated effort was established for failure reporting on tests conducted with flight and prototype hardware and with selected developmental hardware agreed to by the SERT II Project Manager.

Failure reporting

Provisions were established for the organized reporting of failures resulting during selected developmental, acceptance, qualification and life tests, at the component, sub-system and system level. The pertinent information relevant to the failure of the item was furnished to all groups requiring such information.

Failure analysis

The failure analysis of the article was conducted by the appropriate design engineer responsible for the component.

Corrective action resolution

Appropriate corrective action was accomplished on all deficiencies reported on a NASA Failure Report Form. The corrective action was noted as concisely as possible, yet amply detailed, and did denote the required positive action for the resolution of the problem areas.

Review of corrective action activity

Project representatives and R&QAO did jointly participate in periodic engineering review meetings. The purpose of these meeting was to resolve "open" failure and analysis reports, and to define rework, retest, and any additional action necessary to improve and maintain system reliability. A failure, analysis and action report was considered resolved when all concurrence signatures and dates were obtained.

Project summary charts

Dot diagrams were prepared by the Reliability Office for each sub-system. From these diagrams trouble spots can be readily identified and progress toward their solution observed. The pertinent summary information was transmitted to all interested groups.

Performance goal

This Project used as its performance goal a mean-time between-failures for each sub-system greater than 8760 hours. The project data was subjected to weighted statistical analysis to ascertain attainment of the goal by each sub-system. R&QAO did periodically assess the current progress of each sub-system toward meeting the preformance goal.

Equipment log

An equipment log and continuous history on the fabrication, inspection, test, storage and assembly of flight, and prototype components was maintained.

2. Working procedures

The reliability procedures used on the SERT II Project are exhibited and explained in detail in existing literature (14). Procedure 28.0, referenced in Section I.D.3 is given in appendix A to explain a preferred method to ascertain a projects performance toward attaining a previously specified performance goal.

B. MTPC Lift Testing (Problem 23)

Obtaining suitable power-conditioning equipment for electric propulsion units is widely recognized as a critical problem (15). Data have been accumulated on several electric propulsion research projects and other

power-conditioning development contracts which further show that over-stressed electrical parts are a prime cause of equipment failures in electric propulsion experiments.

A typical example of this problem occured during the weightless analysis sounding probe (WASP) fluid dynamic experiment. In this case the failure was in a 28 to 500 volt dc converter which was the power supply for a telemetry transmitter. Failure analysis showed that two, IN 684, subminiature silicon rectifiers had shorted out. Experimental measurements showed that the diodes were not carrying equal amounts of the applied reverse voltage. The other ratings for each diode appeared to be reasonable. The fact that these particular diodes were manufactured with avalanche reverse breakdown properties did not seem to be sufficient protection for long-term, reliable operation under these conditions (16 to 18).

It is generally recognized that component-part failure rates are increasing functions of the stress applied in operation. Furthermore, it is realized that even the best parts, when operated at maximum-rated stress levels, do not have sufficiently low failure rates to allow the synthesis of highly reliable complex systems. Therefore, the need to derate components in application is clearly established (19).

Component derating factors are naturally based on the component reliability at various stress levels. Once the necessary component reliability is established, the maximum stress level at which the component could be operated can be determined without violating the reliability requirement. Unfortunately, curves of reliability as a function of stress exist for only a few components and are generally not well proven even for these. In the remainder of the cases, historical information based on field data obtained from various equipment operating under conditions similar to those of interest must be used.

Table IX shows the recommended derating factors for power conditioners. This table is based on experimental findings and a survey of the best information currently available. Proper use of these derating factors should yield component failure rates in the range 0.1 to 0.001 percent per 1000 hours. Failure rates will also vary widely for different applications because of the particular circuit's tolerance of component drift. Therefore, to ensure low failure rates the designer should strive to achieve the greatest possible circuit tolerance.

Discussion

An electrical stress analysis test was performed on the microthruster power conditioner (MTPC) while it was operating into an adjustable resistive load bank (20). Transient simulation and measurement techniques were worked out. Detailed transient and steady-state data from these measurements are recorded in the (MTPC) equipment log on file at the Lewis Research Center. These data describe some of the response functions that were observed in the test apparatus under worst-case conditions and help explain why the overstress problems were occurring.

Reliability model

The Lewis microthruster reliability model with the interconnection arrangement of the circuits with the thruster is shown in figure 14. Each solid-line box is a necessary component of the sub-system. The dashed line defines the sub-system boundaries. The power conditioner has 27 circuits that are operated by a dc power source. These circuits change the primary power into the proper voltage and currents for the thruster heaters, the high-voltage electrodes, and signals of thruster parameters.

Each component has been assigned an identification number or letter corresponding to the equation index n or j. Numbers were used to identify main component blocks. Lower-case letters were used for auxiliary components. Two equations have been added to this diagram that describe (1) the theoretical reliability of the thruster equipment and (2) the theoretical reliability of the telemetry circuits. This diagram was used as

(1) A basis for redundance

(2) A guide for reliability trade-offs

(3) A guide for failure data reporting and analysis

More complete treatment of reliability models is given in the literature (3, 21).

1. Summary of findings

A summary of the worst-case electrical stress analysis findings is given in table X. The parts have been grouped into six categories. The MTPC equipment contained 523 electrical parts; 52 of these parts had not been derated sufficiently to satisfy recommended derating factors. None of these deficiencies were observed either by calculations or under normal operating conditions. It was necessary to investigate various operating conditions experimentally to find the highest stress conditions. Transients caused by turnon, step changes in parameters, simulated arcs, or turnoff were studied in the laboratory to define these problem areas. Each improper derating condition was analyzed. Corrective design changes were implemented into the breadboard model to eliminate the worst-case overstress conditions.

An examination of the data in table XI reveals that ten UTR 62 rectifiers were overstressed. All of these rectifiers were in output indexes 15 and 16 of the reliability model. Three IN 649 rectifiers were found to be overstressed in indexes 2, 14, and b in figure 14. One IN 746, two IN 1616,

two IN 2999B and eight FD 300 rectifiers were also overstressed, as shown in table XI. In most cases the overstress condition was reverse voltage. In all cases measurements were made for ±V, ±I and W to ensure proper derating under worst-case conditions.

Schematic of index 15

Experimental data for all the electrical parts were obtained by making electrical measurements on the MTPC breadboard. Index 15 for the beam supply is the voltage quadrupler circuit shown schematically in figure 15. The input forcing function $V_{1,i} = V_{2,i}$ is a regulated -24 volts dc. This voltage is applied through an inverter alternately to each half of the primary of T9. The stepped-up output $V_{5,o}$ of T9 is used to charge four quadrupler capacitors, C58 to C62, connected through the rectifiers, CR97 to CR112, to generate +1600 volts dc output, $V_{6,o}$ (22). The table in figure 15 shows the final trim capacitance values that were used in the stress-relieved beam supply.

The UTR 62 rectifiers are alloy-diffused silicon devices. The fabrication process is controlled in such a manner as to optimize recovery time. Fast recovery time suggests that an abrupt junction model is appropriate for these devices. This model is used later to show why proper derating for reverse voltage (-V) is important for long-term reliability.

Test apparatus

The Major piece of test equipment used for these observations was an oscilloscope. One of the more interesting test apparatus setups used to measure rectifier voltage is shown in figure 16. A 200 to 1 attenuator and voltage isolation probe was connected to the test specimen. A logarithmic-scale compression circuit was used to measure the rectifier voltages because of its dynamic range of 4 orders of magnitude. The circuit was

sensitive to test apparatus loading. The differential probe had an input impedance of 30 megohms and 3 picofarads, which appeared to give minimum circuit disturbance. The signal ratio V_{max}/V_{min} was reduced from 600/0.8 to 3/0.004 by the probe. This information is amplified by a factor of 10 to 30/0.04 and fed into logarithmic amplifiers for compression. The voltage across the test specimen was obtained by substracting channel B from channel A. The display device was the oscilloscope.

Ground-loop noises were reduced by connecting the oscilloscope common with the power-conditioner-circuit common and isolating the oscilloscope from its power source.

Unbalance and zero drift are critical adjustments in this dc-coupled measurement technique. Proper attention must be given to each component to assure that it is calibrated, operating, and adjusted properly. Connecting channels A and B to the same point, as a check, assures cancellation of unwanted or interfering signals. It is difficult to resolve $\pm V$ beyond about ±5 percent because of scale compression. However, for dynamic measurements on a system with this complexity, greater accuracy was not required.

Experimental data

Electrical stresses for rectifiers CR97 to CR112 at laboratory ambinet temperature are shown in table XII. The data show that +V, +I, and W meet the requirements of table IX. The measured data at laboratory ambient temperature (approx. 21° C) are compared with the specified spacecraft heat sink at a maximum of 60° C to obtain the pessimistic component derating factor for worse case conditions. Some of the rectifier diodes have reverse voltage and current stresses, -V and -I, with derating factors of 1.0 and 12.5, respectively, which is considerably above the specified deratings.

A P-N junction is reverse recovered from the forward conducting state when the current passing through the junction goes to zero (i.e., righthand thermally generated hole current I_{gp} equals lefthand thermally generated electron current I_{gn}). The junction current goes to zero by diffusion and

drift, removing the majority carriers from the junction. At the instant of switching, a current spike occurs which is the cause for -I to exceed its dc rating by a factor of about 10. The energy rating of the rectifier is not exceeded by these repetitive reverse-current spikes and is, therefore, not a major concern (23 and 24).

Table XII also shows that the junctions were not sharing reverse voltage equally. Appendix B reviews the current theory applicable to junction breakdown to show that equal -V sharing is important for rectifier reliability. For example, CR100 would hold off a potential of 600 volts while CR98 was carrying only 30 volts peak. Based on these observations, it was clear that reliability could be improved if the diodes shared the reverse voltage more equally. In this example, CR97 would pick up about five times more -V when CR100 shorted out than if CR98 shorted out. After a time CR97, which no longer would be properly derated, could fail by this same junction deterioration phenomenon, and thereby, cause CR98 and CR99 to carry the remaining burden with no derating. Eventually all rectifiers would fail and the power-conditioner output would go to zero.

Most probably the part with the greatest electrical stresses will fail first. Past experience with diodes has shown that shorting is the dominant failure mode. If some method could be found to make all reverse potentials nearly equal, a derating factor of about 0.33 could be achieved, and the probability of junction deterioration breakdown occurring could be reduced.

Conventional methods were employed to improve reverse-voltage sharing as this could possible have improved the long-term reliability of a series of rectifiers (17 and 18). The circuit stopped operating properly when these different methods were tried.

Recognizing that equal junction capacitance terms would share reverse voltages equally, three fixed trim capacitors were added to each string to meet the desired constraint $0.9 \leq -V \leq 1.1$ V. In figure 15 the arrangement of trimmer capacitors and their values are shown. Table XIII shows

that quite an improvement in -V has been accomplished by adding the proper capacitance without affecting -I appreciably. The maximum spread on uncompensated reverse voltage of 17 to 600 volts peak has been reduced to 160 to 205 volts peak (compare table XII with table XIII).

Reverse voltage may have exceeded the desired tolerance by a small amount; however, the tolerance was primarily determined by the fixed values of mica capacitors available. Reverse current has been increased roughly by a factor of 2. This is not nearly enough to influence the energy rating W or circuit operating parameters. It remained to show that temperature would not adversely influence voltage sharing and that such a rectifier string would operate for a long time without failure.

Temperature data for I and V were taken by placing the rectifiers, CR97 to CR112, and trim capacitors in a temperature chamber. Ten temperatures spaced approximately 14^{o} C apart in the range from -54^{o} to 85^{o} C were selected as test points. The test data for $\pm I$ and $\pm V$ did not show that temperature has any pronounced effect on the circuit response. Table XIII summarizes the data for -V by giving the central value μ_{-V}, and standard deviation σ_{-V}, in the test temperature range.

The mean value of reverse voltage varies from 162 with $\sigma_{-V} = 7.7$ volts peak to 209 with $\sigma_{-V} = 5.8$ volts peak. Analytical consideration of figure 15 helps explain why temperature has very little influence on voltage sharing for this compensation method. The transformer T9 has been optimized for weight, which tends to increase copper losses; copper, silicon, and mica all have positive changes in resistance, leakage, and capacitance, with temperature. When these two facts are considered, one explanation for this nominal temperature effect may be that as temperature increases the copper losses increase. At the same time the load impedance is decreasing, which tends to maintain a constant response function. Conversely, when temperature decreases the copper losses decrease and the load impedance increases, which tends to hold $V_{6,o}$ constant.

Exhibited response

The microthruster power-conditioning breadboard revised to eliminate high-stress areas was run in the laboratory without failure for 7052.3 hours. The laboratory apparatus was shutdown at this time, for the previously selected mean-time-between failures of 4320 hours had been exceeded by about 60 percent and the laboratory space was needed for a new task.

2. Conclusions and recommendations

The worst-case electrical stress analysis test performed on a microthruster power-conditioning breadboard disclosed a number of electrical parts which were overstressed. Each overstressed part was analyzed to determine suitable corrective action. Corrective design changes were implemented into the breadboard model.

Experimental measurements showed that a worst-case stress analysis obtained through laboratory testing is necessary to identify overstressed conditions which are not evident from an analytical study or from subjecting the equipment to normal operating conditions. The rectifier diode problem is an example of a worst-case stress condition that was identifiable only through laboratory testing. As a result of this testing, the rectifier problem was solved by adding high-reliability mica capacitors across the rectifiers to improve the voltage sharing capabilities of this design.

Breakdown theory shows that junction deterioration could have been the cause of several critical failures which have occurred on past ion-engine research projects. A further review of these breakdown theories showed that avalanche construction is not always the answer to obtaining long-term reliable operation under a repeated transient condition.

An ion-thruster power conditioner was modified to eliminate the evidenced over-stressed conditions described herein. This power conditioner operated properly for more than 7000 hours. This life test results supported the LeRC contention that electric rockets were ready for long term space testing; thus paving the way for SERT II.

APPENDIX A

PERFORMANCE GOAL

1. Purpose

To ascertain the SERT II Project performance for each sub-system toward attaining a previously specified performance goal.

2. Reference document

Provision No. 2.8, Performance Goal

3. Recommended steps to calculate a sub-system performance goal

(a) Review the failure array data and prepare the tabulated column data for t_j, w_j and f_i (see term definitions listed below).

(b) Calculate the $\bar{t}_{PG}$ for each subsystem. The weighting equation for $\bar{t}_{PG}$ is given by,

$$\bar{t}^{x}_{PG} = \frac{\sum_{j=1}^{n} w_j t_j}{\sum_{i=1}^{n} f_i}$$

where

$\bar{t}_{PG}$ performance goal (MTBF, hr/F) for the xth sub-system

t_j operating time of the xth sub-system (hours)

w_j per unit xth sub-system weighting factor (pure number)

f_i number of failures of the xth sub-system (failures)

APPENDIX B

JUNCTION BREAKDOWN FOR RECTIFIER RELIABILITY

Presently there are two theoretical explanations as to how a P-N junction which has voltage applied in the reverse direction abruptly changes from high to essentially zero resistance. Figure 17 shows these two types of breakdown. Both types of breakdown have been observed on an oscilloscope in the laboratory.

From the origin to point A, the reverse current appears to be following the theoretical diode equation (23),

$$I = I_S\left[\exp\left(\frac{qV}{kT} - 1\right)\right] \tag{1}$$

and

$$I_S = I_{gp} + I_{gn}$$

From A to B, -I is increased by a leakage component. From B to E, there are two apparent paths by which breakdown occurs. These paths B-C-E and B-D-E are often referred to as the Zener and Townsend breakdown paths, respectively. The actual breakdown mechanisms are not well understood as each theory does not fit exactly with the observed phenomena.

The Zener breakdown theory postulates that the covalent bonds in the vicinity of the depletion are spontaneously disrupted by the high electric fields that exist in this region (25). The carriers made available by the disrupted bonds would add to I_{gp} and I_{gn}. For high fields, large numbers of field carriers would be generated, limited only by the external circuit resistance, taking -I into the E-F or avalanche region (26 and 27).

High fields are certainly present in P-N junctions under reverse bias conditions, as can be seen from the following simplified analysis. The experimentally studied rectifiers were UTR 62 devices with fast recovery

time. Figure 18 shows an abrupt junction model which is appropriate for these devices. Since $x = W_1 + W_2$ and $\xi = 0$ (fig. 18), a point of inflection occurs at $x = 0$ and ξ is maximum (23); therefore,

$$\xi_{max} = \frac{qN_d}{\epsilon} W_2$$

For an abrupt junction,

$$\xi_{max} = \left(\frac{2V_B}{\epsilon \mu_n P_n} \right)^{1/2}$$

For silicon this becomes,

$$\xi_{max} \simeq 6.3 \times 10^4 \left(\frac{V_B}{P_n} \right)^{1/2} \qquad (2)$$

where

$$P_n = 5.0\ \Omega\text{-cm}$$

$$V_B = V_{eq} - V, \quad V_{eq} \ll V$$

Therefore,

$$V_B \simeq |-V| = 200 \text{ volts}$$

and

$$\xi_{max} = 3.98 \times 10^5 \text{ volts/cm}$$

Even thouth this analysis is only approximate, it is clear that this is a very high field and spontaneous disruption of the covalent bonds is quite likely. However, due to the inability of this theory to explain some observable phenomena, it is no longer accepted as complete.

The Townsend breakdown theory (28) develops the analog between a gas discharge and a P-N junction breakdown. The reverse junction current is

composed of thermally generated holes, electrons, and leakage (eq. (1) and fig. 17). When the applied junction potential is increased, from point B, -V increases the energy state to a point where the thermal carriers begin to experience ionizing collisions. Each ionizing collision contributes secondary holes and electrons to -I, beyond the leakage contribution. This causes carrier multiplication to occur, as each ionized carrier may strike several atoms as it passes through the depletion zone. Depending on the magnitude of the applied potential -V, the number of ionizing collisions can cascade quite rapidly as shown along the path B-D-E (fig. 17). From point E upward, the number of carriers generated by collision is no longer a function of -V, as V_A has been reached. The junction current is, in the E-F region, again, only limited by the external circuit resistance.

It can be seen that all P-N junctions will avalanche at some potential. Whether this disturbance occurs along path B-D-E or B-C-E does not change the fact that this is a very high stress condition for any junction and can easily cause failure. It has been shown in the literature (16 to 18) that the instantaneous energy rating cannot be exceeded, or sudden failure by punch-through will occur. The fact that a particular P-N junction can operate in the E-F region under controlled conditions by virtue of avalanche construction does not give total assurance against deterioration due to repeated high reverse-voltage stresses.

Elevating the temperature in which the junction operated aggravates the situation still further. Temperature causes I_S to increase. For silicon, I_S increases about 1 order of magnitude for each 20 K. This increase would suggest that since the number of carriers has increased, the avalanche potential V_A should decrease. Here, both theories appear to be misleading, as in many cases the measured value of V_A increases slightly with temperature.

It appears that the Early effect (29) under certain conditions may cause deterioration in P-N junctions. This may explain why P-N junctions that were avalanche protected still suffered gradual deterioration as a result of high reverse-voltage stress. This potentially unreliable condition can be minimized by adding a small trimmer capacitor across each exposed junction to cause equalization of reverse voltage.

REFERENCES

1. Anon.: Reliability Theory and Practice. ARINC Res. Corp., Washington, D.C., 1962.
2. Anon.: Reliability By Design. General Electric Co., Defense Elect. Div., Waynesboro, Va., 1964.
3. Bazovsky, Igor: Reliability Theory and Practice. Prentice-Hall, Inc., 1961.
4. Earles, D. R.; and Eddins, M. F.: Reliability Physics. AVCO Corp., Wilmington, Mass., 1962.
5. Calabro, S. R.: Reliability Principles and Practices. McGraw-Hill Book Co., Inc., 1962.
6. Berretonni, J. N.: Practical Application of the Weibull Distribution. Am. Soc. Quality Control Conference Transactions, 1962.
7. Anon.: Failure Distribution Analyses Study. Vols. I, II, and III. Computer Applications Inc., Aug., 1964.
8. Hoel, Paul G.: Elementary Statistics. John Wiley & Sons, Inc., 1960.
9. Lochner, R. H.: When and How to Use the Weibull Distribution. Reliability Res. and Ed. Dept., General Motors Corp., Milwaukee, Wisc., 1963.
10. Lochner, R. H.: Estimation and Prediction Using the Binomial Distribution. Reliability Res. and Ed. Dept., General Motors Corp., Milwaukee, Wisc., 1963.
11. Leone, F. C., et al.: Percentiles of the Binomial Distribution. Case Institute of Technology, 1967.
12. Lochner, R. H.: Reliability Calculations for Exponential Population. Reliability Res. and Ed. Dept., General Motors Corp., Milwaukee, Wisc., 1963.
13. Anon.: Descriptive Statistics. IEEE Statistics Course at Case Western Reserve Univ., Spring 1963.

14. Anon.: SERT II Reliability & Quality Assurance Manual. R&QA Office, NASA Lewis Research Center, Cleveland, Ohio.

15. Anon.: Propulsion. Space/Aeronautics, Res. & Dev. Tech. Handbook, vol. 44, no. 2, 1965-66, p. 49.

16. Hitchcock, R. C.: Avalanche Diodes: The Answer to High PRV. Electronic Des., vol. 12, no. 17, Aug. 17, 1964, p. 166.

17. Gutzwiller, F. W.: Rectifiers in High Voltage Power Supplies. Electronic Design, July 23, 1958.

18. Von Zastrow, E. E.: Voltage Failures in Series-Connected Diodes - Their Cause and Prevention. Electronic Des., vol. 13, no. 22, Oct. 25, 1965, p. 62.

19. Anon.: JPL Preferred Parts List - Reliable Electronic Components. Spec. ZPP-2061-PPL-H. Jet Propulsion Lab., Calif. Inst. Tech., July 1, 1966, table VI.

20. Kotnik, J. Thomas; and Sater, Bernard L.: Power-Conditioning Requirements for Ion Rockets. IEEE Trans. on Aerospace, vol. As-2, Apr. 1964, pp. 496-504.

21. Lalli, Vincent R.: Ion Engine Subsystem Reliability Procedure. Proceedings of the 11th National Symposium on Reliability and Quality Control. IEEE, 1965, pp. 361-379.

22. Smith, Fritz L., ed.: Radiotron Designer's Handbook. Fourth ed., Radio Corp. of America, 1953.

23. DeWitt, David; and Rossoff, Arthur L.: Transistor Electronics. McGraw-Hill Book Co., Inc., 1957.

24. Shockley, W.: The Theory of P-N Junctions in Semiconductors and P-N Junction Transistors. Bell Sys. Tech. J., vol. 28, no. 3, July 1949, pp. 435-489.

25. McAfee, K. B.; Ryder, E. J.; Shockley, W.; and Sparks, M.: Observations of Zener Current in Germanium P-N Junctions. Phys. Rev., vol. 83, no. 3, Aug. 1, 1951, pp. 650-651.

26. McKay, K. G.; and McAfee, K. B.: Electron Multiplication in Silicon and Germanium. Phys. Rev., vol. 91, no. 5, Sept. 1, 1953, pp. 1079-1084.

27. McKay, K. G.: Avalanche Breakdown in Silicon. Phys. Rev., vol. 94, no. 4, May 15, 1954, pp. 877-884.

28. Cobine, James D.: Gaseous Conductors, Theory and Engineering Applications. Dover Publications, 1958.

29. Early, J. M.: Effects of Space-Charge Layer Widening in Junction Transistors. Proc. IRE, vol. 40, no. 11, Nov. 1952, pp. 1401-1406.

TABLE I. - FIT DATA FOR FAILURE FUNCTIONS

Distribution (continuous)	Times to failure fit
1. Exponential	Complex electrical systems
2. Normal	Mechanical systems subject to wear
3. Weibull	Mechanical, electromechanical or electrical parts: bearings, linkages with fatigue loads, relays, capacitors, semiconductors. Reduces to distribution 1 if $\alpha = t$, $\beta = 1$, and $\alpha = 0$
4. Gamma	Combined mechanical and electrical systems
5. Log normal	Mechanical parts under stress rupture loading
(discrete)	
6. Poisson	One shot parts
7. Binomial	Complex electrical systems for probability of N_f defects

TABLE II. - TEST DATA FOR

GIMBAL ACTUATORS

Ordered sample number	t_f, K hr	t_f^2, $(\text{K hr})^2$
1	60	3600
2	65	4225
3	68	4624
4	70	4900
5	75	5625
6	75	5625
7	80	6400
8	83	6889
9	85	7225
10	90	8100
Totals	750	57 213

TABLE III. - WEIBULL DATA FOR STEPPING MOTORS

Number of steps to failure $\times 10^{-3}$	Cumulative number of failures		Median rank	5 Percent rank	95 Percent rank
	Problem 3	Problem 9			
0.2	2	1	6.70	0.51	25.89
.4	4	2	16.23	3.68	39.42
.9	5	3	25.86	8.73	50.69
4.0	16	4	35.51	15.00	60.66
10.0	20	5	45.17	22.24	69.65
18.0	50	6	54.83	30.35	77.76
30.9	90	7	64.49	39.34	85.00
50.0	97	8	74.14	49.30	91.27

TABLE IV. - ELECTRIC ROCKET RELIABILITY DATA

Ordered sample number	Time-to-failure hr	Median rank	Scaled time-to-failure	Linear scaled ranks
1	1 037.8	6.70	7.2	5.0
2	1 814.4	16.23	12.6	15.0
3	2 332.8	25.86	16.2	25.0
4	3 124.8	35.51	21.7	35.0
5	3 614.4	45.71	25.1	45.0
6	4 579.2	54.83	31.8	55.0
7	5 342.4	64.49	37.1	65.0
8	6 292.8	74.14	43.7	75.0
9	7 920.0	83.77	55.0	85.0
10	11 404.8	93.30	79.2	95.0

TABLE V. - TEST DATA FOR GUY SUPPORTS

Ordered sample number	Time-to-failure, hr	Median rank	5 Percent rank	95 Percent rank
1	1 100	6.7	0.5	25.9
2	1 890	16.2	3.7	39.4
3	2 920	25.9	8.7	50.7
4	4 100	35.5	15.0	60.7
5	5 715	45.2	22.2	69.7
6	8 720	54.8	30.3	77.8
7	12 000	64.5	39.3	85.0
8	17 500	74.1	49.3	91.3
9	23 900	83.3	60.6	96.3
10	46 020	93.3	74.1	99.5

TABLE VI. - POISSON DATA FOR

SPEED CONTROLLER

Ordered sample number	Time-to-failure, hr
1	3 520.0
2	4 671.2
3	6 729.3
4	7 010.0
5	8 510.2
6	9 250.1
7	10 910.0
8	11 220.5
9	11 815.6
10	12 226.4
Total	85 866.3

TABLE VII. - BINOMIAL COEFFICIENTS

Sample size	Possible failure	Binomial coefficients
1	2	1
2	3	1 2 1
3	4	1 3 3 1
4	5	1 4 6 4 1

TABLE VIII. - ADVANCED-STRESS TESTING GUIDELINES

1. Define the multidimensional stress region for an item; nominal values should be centrally located.
2. Study the failure mechanisms applicable to this item.
3. Based on items 1 and 2 decide which stresses can be advanced without changing the failure mechanisms.
4. Specify multiple stress tests to establish trends; one point should be on the outer surface of the multidimensional region.
5. Be sure that the specimen size at each stress level is adequate to identify what the failure density functions are and that it has not changed from level to level.
6. Pay attention to the types of failures that occur at various stress levels to be sure that new failure mechanisms are not being introduced.
7. Do new techniques that are being developed for advanced-stress testing apply to this item? Several popular techniques are described below:
   a. Sensivity testing - Test an item at the boundary stress for a given time. If failure occurs, reduce stress by a fixed amount and retest for the same time. If no failure occurs, increase stress by a fixed amount and retest for the same time. Repeat this process until 25 failures occur. This technique is used to define endurance limits for items.
   b. Least-of-N Testing - Cluster items in groups, subject each cluster to a specified stress for a given time. Stop at the first failure at each stress level. Examine failed items to insure conformance to expected failure mechanisms.
   c. Progressive-Stress Testing - Test an item by starting at the central region in stress space and linearly accelerate stress with time until faliure occurs. Observe both the failure stress level and rate of increase of stress. Vary the rate of increasing stress and observe its effect on the failure stress magnitude. Examine failed items to insure conformance to expected failure mechanics.

TABLE IX. - COMPONENT DERATING FACTORS FOR POWER CONDITIONERS

Component	Derating factor[a]	Component derating weighting factors		Stress	Remarks
		X	Y		
Capacitors				Voltage	The following equation establishes the derating factor for capacitors where values of X and Y are given: Derating factor = $X - \frac{C - C_{min}}{C_{max} - C_{min}} (Y)$ where C capacitance value of capacitor for which derating factor is desired; C_{min} smallest capacitance value available with same case size and voltage rating as C; C_{max} largest capacitance value available with same case size and voltage rating as C
Ceramic disc	0.7	---	---		
Ceramic, low voltage	---	0.5	0.2		
Glass:					
CYFR10 and CYFR15	0.7	---	---		
CYFR20 and CYFR30	.5	---	---		
Porcelain	---	0.7	0.2		
Mica	---	.7	.2		
Plastic film	---	.5	.2		
Paper	---	.8	.1		
Metalized	---	.5	.2		
Tantalum, solid	---	.7	.3		
Tantalum, wet slug and foil	0.7	---	---		
Connectors, low voltage	---	---	---	Current	Contacts shall be derated to 75 percent of rating for individual contacts. The average current rating from 1 to 15 contacts shall be decreased linearly to 20 percent. For more than 15 contacts the rating is 20 percent of the normal individual contact rating. The applied voltage between contacts or between contacts and shell shall not exceed 250 volts rms.
Silicon diodes					Current and voltage derating factors shall be applied simultaneously.
Signal and switching	0.6	---	---	+I	
	.5	---	---	+V, -I	
	.3	---	---	$\overline{W}$	
Power ($I_o \leq 10A$)	.85	---	---	+I	
	.5	---	---	+V, -I	
	.43	---	---	$\overline{W}$	
Power ($10A < I_o \leq 35A$)	.75	---	---	+I	
	.5	---	---	+V, -I	
	.38	---	---	$\overline{W}$	
Zener (power $\leq$ 1W)	.5	---	---	Power	
Zener (1W < power $\leq$ 50W)	.5	---	---	Power	
Microcircuits	---	---	---	-------	Supply voltages may be reduced to effect lower power consumption, at the price of slower switching speeds and narrower noise-immunity margins. Allowable fan-out should be reduced for reliable operation. Operation over wide temperature ranges will generally result in decreased circuit margins and fan-out capability. Operational stability may be improved if power-supply voltage tolerances are tightened, especially if the devices employ non-saturating circuitry.
Relays	0.3	---	---	Current	----------
Resistors				Power	----------
Composition	0.7	---	---		
Film	.4	---	---		
Wirewound power	.5	---	---		
Wirewound precision	.4	---	---		
Transformers	0.4	---	---	Power	----------
Silicon transistors	.25	---	---	Power	Voltage applied across any junction or group of junctions shall not exceed 50 percent of rated voltage

TABLE X. - STRESS ANALYSIS

FINDINGS

Component	Total used	Overstressed[a]
Rectifiers	167	26
Transistors	84	9
Capacitors	91	10
Resistors	170	2
Transformers	9	4
Relays	2	1
Total	523	52

[a]Percentage of parts overstressed, 9.9 percent.

TABLE XI. - OVERSTRESSED-RECTIFIER

DETAILS

Schematic symbol	Measured derating factor[a]	Type	Model location (fig. 14)
81, 84, 101	0.80	UTR 62	16
85	1.08	↓	16
89, 93	.93	↓	16
100, 108	1.00	↓	15
109	.63	↓	15
112	.73	↓	15
7	.97	IN 649	2
22	1.74	↓	b
37	5.18	↓	14
113, 114	Spikes	IN 1616	10
54	.97	IN 746	17
8, 9	.79	IN 2999B	10
14, 15	Spikes	FD 300	4
134, 135, 137	↓	↓	11
146, 147	↓	↓	8
165	↓	↓	2

[a]The specified derating factor for working inverse voltage as given in table I is 0.50.

TABLE XII. EXHIBITED RECTIFIER DATA

Rating at, 60° C	600	1.1 at 1A	1600	0.07 at 600 V	105
Schematic symbol	Reverse voltage, -V, (volts)	Voltage, V, (volts)	Current, I, (mA)	Reverse current, -I, (mA)	Energy rating, W, (watt-sec×10^4)
CR 97	62	0.59	3.8	0.9	0.14×10^4
98	30	↓	↓	↓	.07
99	56	↓	↓	↓	.13
100	600	↓	↓	↓	1.4
101	480	.63	8.0	↓	1.1
102	48	↓	↓	↓	.11
103	52	↓	↓	↓	.12
104	240	↓	↓	↓	.55
105	40	.69	20.0	0.8	.08
106	17	↓	↓	↓	.03
107	28	↓	↓	↓	.06
108	600	↓	↓	↓	1.2
109	380	↓	17.0	↓	.76
110	64	↓	↓	↓	.13
111	58	↓	↓	↓	.11
112	440	↓	↓	↓	.88

TABLE XIII. - COMPENSATED RECTIFIER DATA

Temperature, °C	21		-54 to 85	
Schematic symbol	Reverse voltage, -V, (volts)	Reverse current, -I, (mA)	Mean reverse voltage, $-\overline{V}$, (volts)	Standard deviation, σ, (volts)
CR 97	205	1.7	209	5.8
98	200	↓	195	4.7
99	175	↓	172	5.8
100	205	↓	209	4.7
101	190	1.6	195	4.7
102	178	↓	173	7.7
103	170	↓	179	7.7
104	190	↓	198	7.1
105	160	↓	171	7.7
106	162	↓	172	5.8
107	180	↓	183	4.7
108	190	↓	196	5.8
109	192	1.4	201	4.7
110	165	↓	169	4.7
111	160	↓	162	7.7
112	175	↓	179	7.1

Distribution	f(t)	R(t)	λ	λ'	Remarks
1. Exponential	$\frac{1}{\bar{t}} \exp[-t/\bar{t}]$	$\exp[-t/\bar{t}]$	$\frac{1}{h}\left\{1 - \frac{\exp[-t_2/\bar{t}]}{\exp[-t_1/\bar{t}]}\right\}$	$1/\bar{t}$	$h = t_2 - t_1$
2. Normal	$\frac{1}{\sigma\sqrt{2\pi}} \exp[-(t-\bar{t})^2/2\sigma^2]$	$\frac{1}{\sigma\sqrt{2\pi}} \int_t^\infty \exp[-(t-\bar{t})^2/2\sigma^2]dt$	$\frac{1}{h}\left[1 - \frac{R(t_2)}{R(t_1)}\right]$	$\frac{\text{Normal ordinate at } t}{\text{Normal area } t_1 \text{ to } \infty}$	
3. Weibull	$\frac{\beta}{\alpha}(t-\gamma)^{\beta-1} \exp\left[\frac{-(t-\gamma)^\beta}{\alpha}\right]$	$\exp -(t-\gamma)^\beta/\alpha$	$\frac{1}{h}\left\{1 - \frac{\exp[-(t_2-\gamma)^\beta/\alpha]}{\exp[-(t_1-\gamma)^\beta/\alpha]}\right\}$	$\frac{\beta}{\alpha}(t-\gamma)^{\beta-1}$	α = scale parameter β = shape parameter γ = location parameter
4. Gamma	$\frac{1}{\alpha^\beta \Gamma(\beta)}(t-\gamma)^{\beta-1} \exp[-(t-\gamma)/\alpha]$	$\frac{1}{\alpha^\beta \Gamma(\beta)} \int_t^\infty (t-\gamma)^{\beta-1} \exp[-(t-\gamma)/\alpha]dt$	$\frac{1}{h}\left\{1 - \frac{(t_2-\gamma)^{\beta-1}\exp[-(t_2-\gamma)/\alpha]}{(t_1-\gamma)^{\beta-1}\exp[-(t_1-\gamma)/\alpha]}\right\}$	$\frac{\text{Gamma ordinate at } t}{\text{Gamma area } t_1 \text{ to } \infty}$	Gamma functions $\Gamma(\beta) = \int_0^\infty t^{\beta-1}e^{-t}\,dt$ Recurrence form $\Gamma(\beta) = (\beta-1)\Gamma(\beta-1)$ $\Gamma(1) = \Gamma(2) = 1$
5. Log normal	$\frac{1}{t'\sigma_{t'}\sqrt{2\pi}} \exp\left[-\frac{1}{2}\left(\frac{t'-\bar{t}'}{\sigma_{t'}}\right)^2\right]$	$\frac{1}{\sigma_{t'}\sqrt{2\pi}} \int_{\log_e(t)}^\infty \exp\left[-\frac{1}{2}\left(\frac{t'-\bar{t}'}{\sigma_{t'}}\right)^2\right]dt'$	$\frac{1}{h}\left[1 - \frac{R(t_2)}{R(t_1)}\right]$	$\frac{\text{Log normal ordinate at } t}{\text{Log normal area } t_1 \text{ to } \infty}$	
	$f(N_f)$	$R(N_f)$			
6. Poisson	$\frac{(t/\bar{t})^{N_f} \exp[-t/\bar{t}]}{N_f!}$	$\sum_{j=N_f}^{n} \frac{(t/\bar{t})^j \exp[-t/\bar{t}]}{j!}$	Not applicable	Not applicable	p = defectives q = effectives n = trials (sample size) N_f = number of failures
7. Binomial	$\frac{n!}{(n-N_f)!N_f!} p^{N_f} q^{n-N_f}$	$\sum_{j=N_f}^{n} \frac{n!}{(n-j)!j!} p^j q^{n-j}$	Not applicable	Not applicable	

Figure 1. - Summary of useful frequency functions.

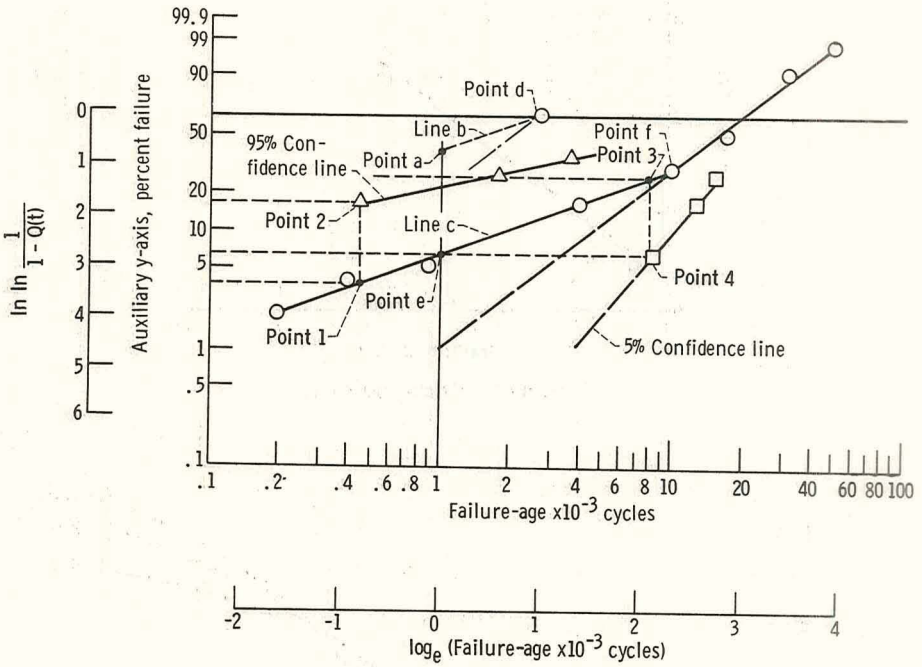

Figure 2. - Weibull plot for stepping motors.

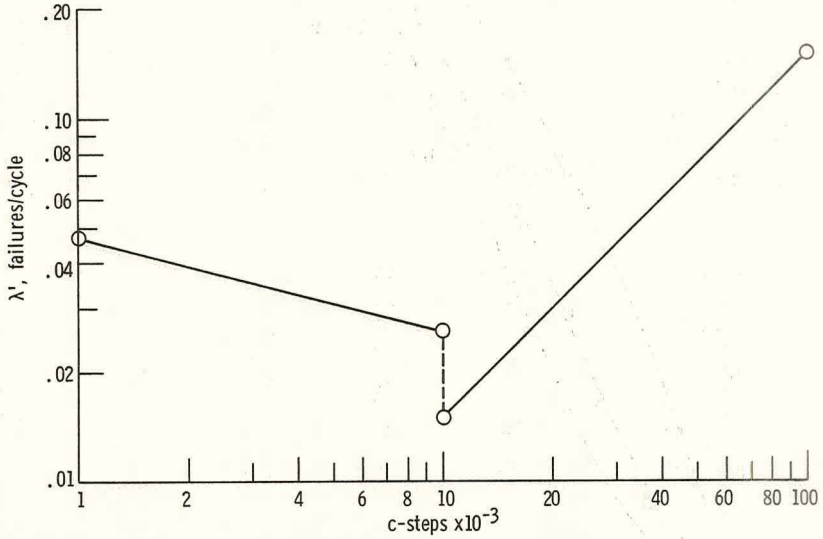

Figure 3. - Hazard rate graph for stepping motors.

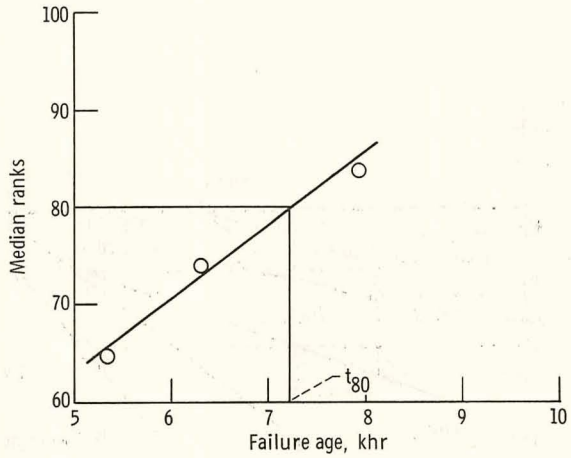

Figure 4. - Electric rocket life.

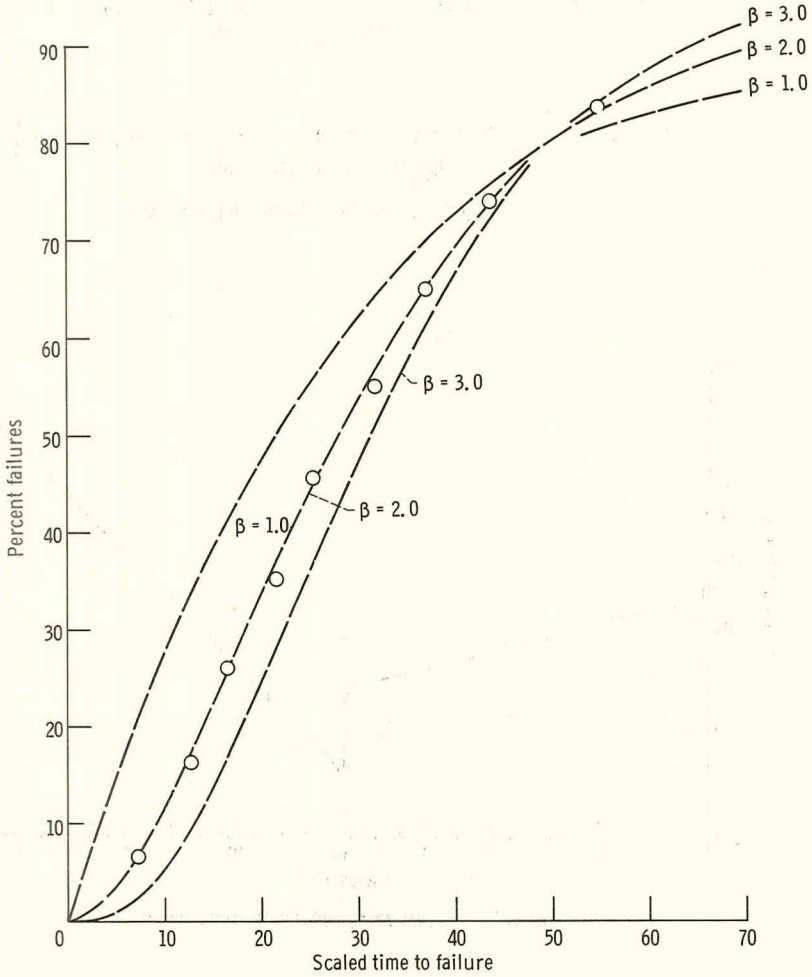

Figure 5. - Electric rocket β parameter curves.

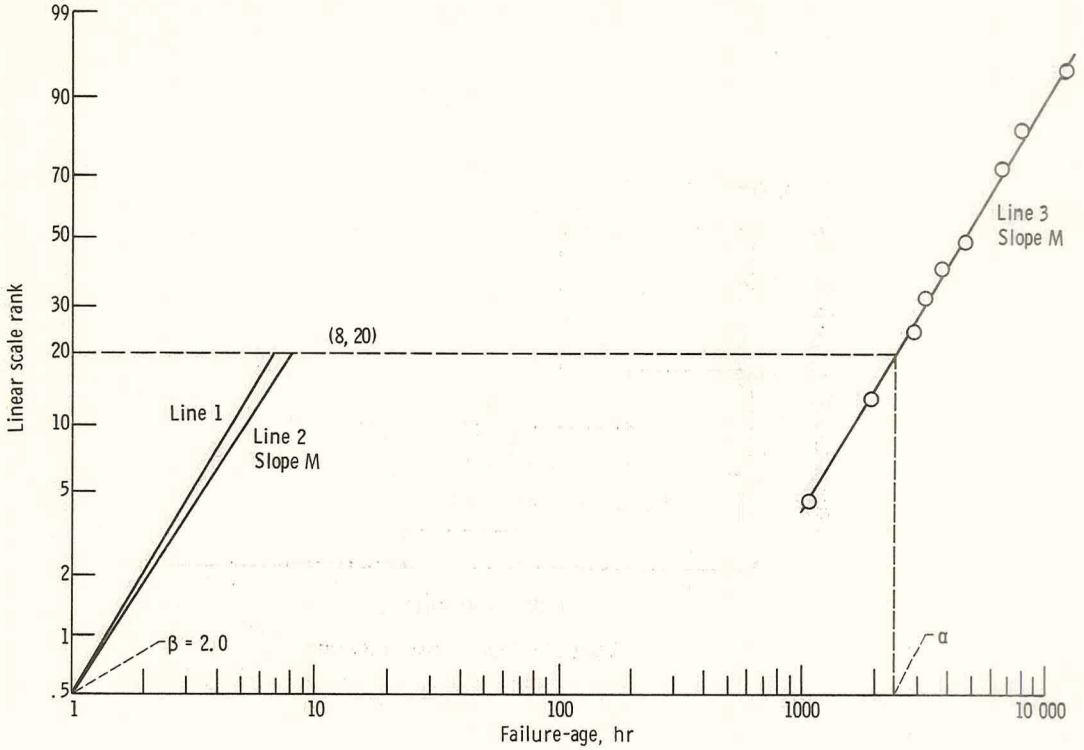

Figure 6. - Electric rocket and parameter diagram.

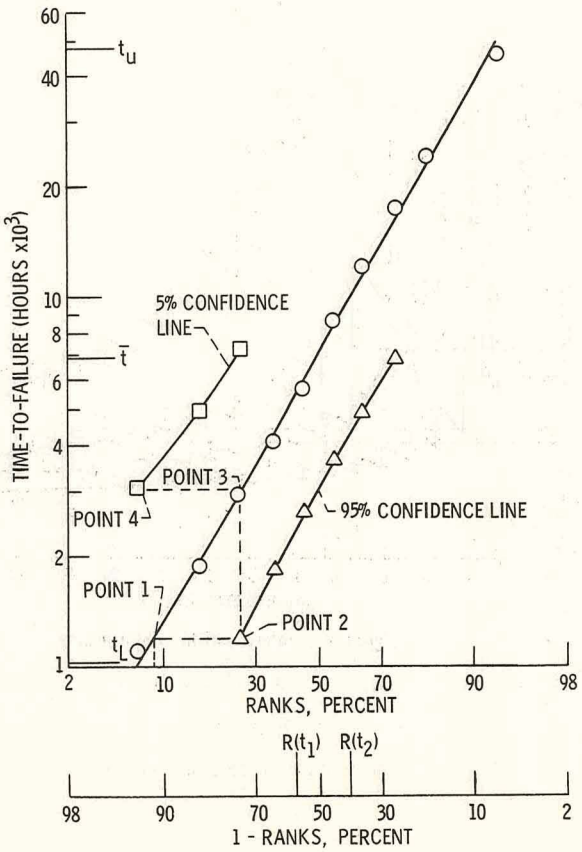

Figure 7. - Guy support life.

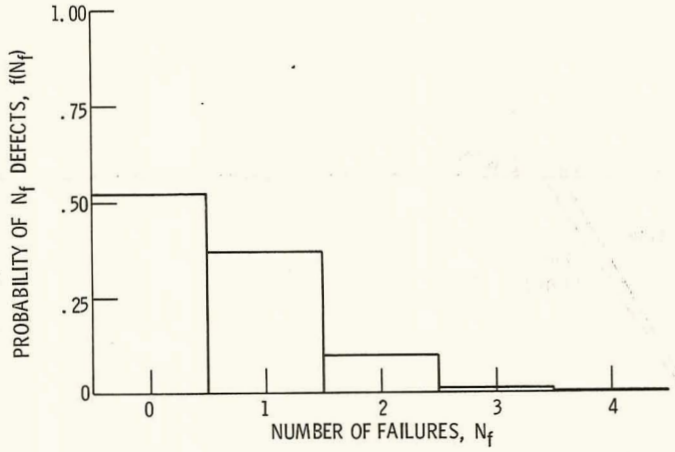

Figure 8. - Explosive bolts histogram.

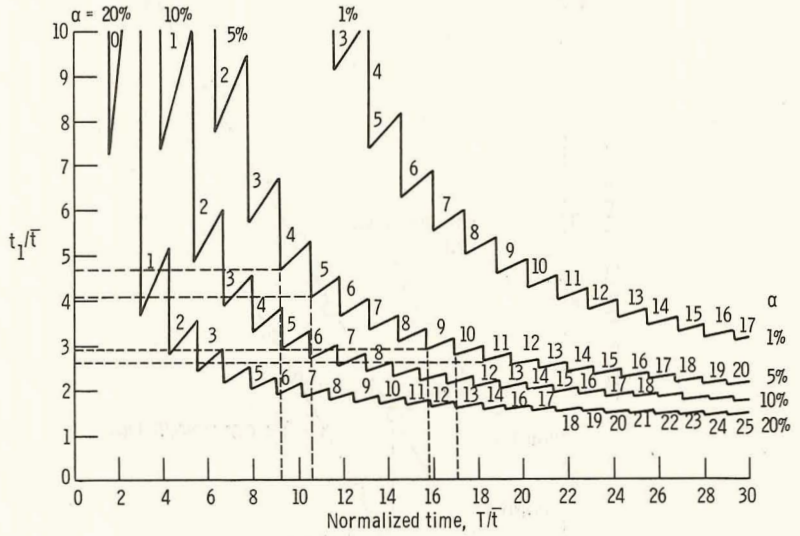

Figure 9. - Poisson MTBF fixed test time.

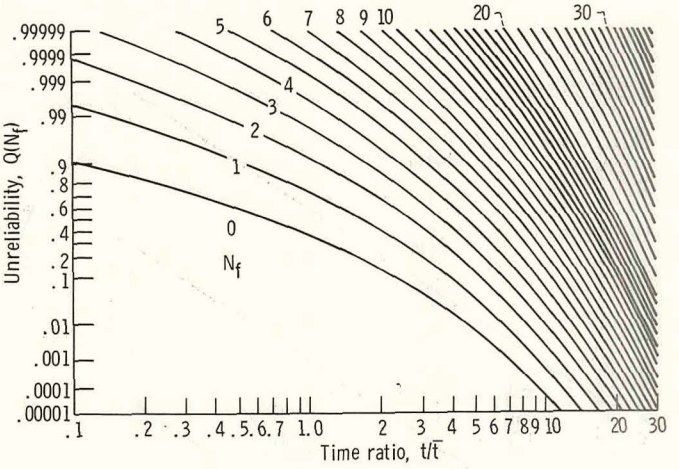

Figure 10. - Poisson unreliability sum.

6433	2582	0820	1460	6606	7143	9158	5114	9491	8063
3465	7348	5774	3821	6216	2148	1221	5895	7942	9971
9601	9189	0141	1377	3467	7971	0811	8309	0504	4606
2364	3260	1430	9505	3146	4815	9732	3447	7705	4532
7304	9292	4580	8160	7144	8073	8476	1896	6661	1285
3764	5460	6385	9045	7170	5831	4668	9386	3979	1116
0251	3139	4201	0578	2172	6876	4347	4288	1514	9985
2031	0919	7613	1535	1610	7491	3255	4014	3614	5599
6398	1374	1904	7490	3941	0284	5817	1630	4629	6773
0911	3930	0324	8151	3365	6685	0566	5047	8471	6166
5052	5023	3045	3433	6365	7310	5073	5416	2332	0922
9225	3984	4659	4642	7260	1383	7625	7512	8547	7343
3100	7916	9757	8869	5307	2691	0786	2701	0102	5745
4598	0065	4257	6557	4638	8418	7398	9790	5074	8018
5956	7285	0480	1411	7766	3377	5023	0227	8047	1887
9360	1041	2094	4212	2623	2384	6422	5374	0651	8673
8796	9974	1913	8309	4943	9423	9143	4683	4436	8413
7071	8254	6825	3020	9000	4673	6129	0176	3670	4836
7336	4451	5863	6559	5344	0714	1856	0451	7855	5998
1660	0222	2005	0215	2370	2687	3039	7953	1960	6579
7506	1020	8718	9665	1892	8245	7249	6023	4602	4227
5000	8237	6203	6829	5325	5784	8720	5053	6347	1112
4255	6894	8093	9191	5011	0452	6199	0009	8086	5170
5764	9837	6780	7490	5412	4869	6950	4183	8671	4008
3609	1368	9129	7113	3099	1887	0544	6415	9148	4381
7218	5939	4932	5465	6648	6365	4179	9266	9803	5572
6854	5911	1495	4940	4630	4514	0942	7218	7382	2145
4403	4263	4755	5451	8251	2652	6207	4841	3528	7665
2978	4381	2205	9638	6946	7126	9039	9194	6676	4396
1072	2292	4428	4934	8183	7385	3236	7748	4488	1351
6488	6568	9530	8316	7709	9022	8041	5564	6667	5329
9263	7756	6300	6793	7769	3099	3606	2468	2574	5230
0357	3493	0385	4451	4313	3024	8243	4920	3523	9644
5372	9351	8393	6023	2811	1744	2306	7083	4330	7278
6570	2866	7565	7871	9490	9050	4454	3475	8319	2972
8596	8251	0336	8119	1966	9115	4202	7785	5269	5941
4177	0092	4207	7386	9891	1149	3429	7062	4622	8415
8438	4892	2089	5509	2054	9024	1213	5791	2543	7863
5820	6287	7484	0339	8585	0968	3675	2440	4000	5148
7721	3804	9520	6184	9152	1853	8640	3601	5606	7218

Figure 11. - Random digits table.

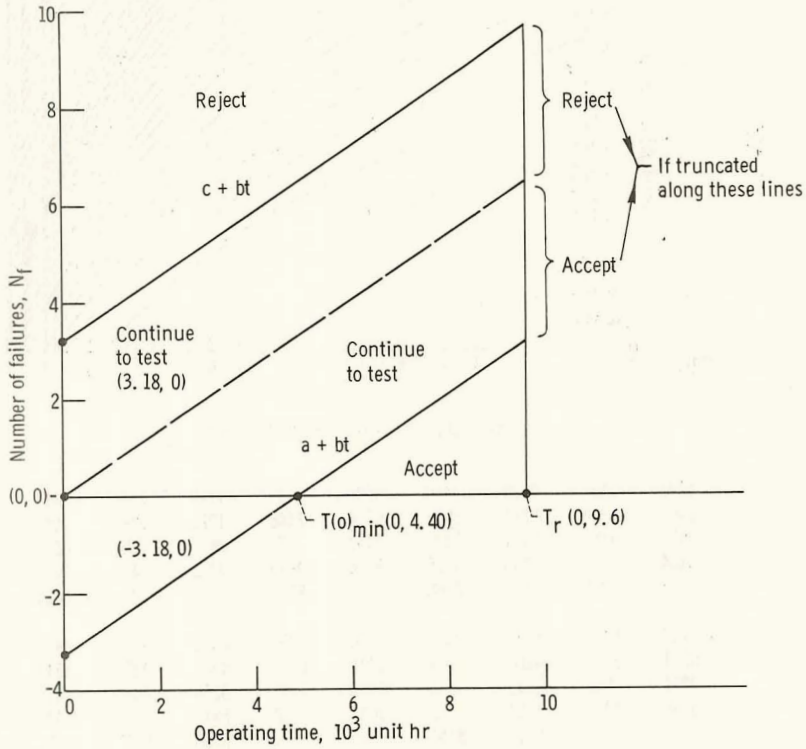

Figure 12. - Tantalum capacitors reliability chart.

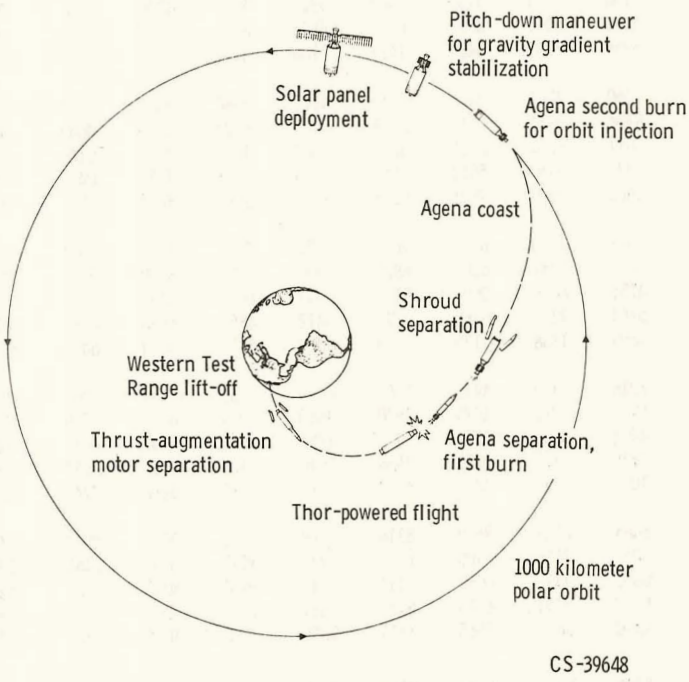

Figure 13. - Representation of Sert II flight sequence.

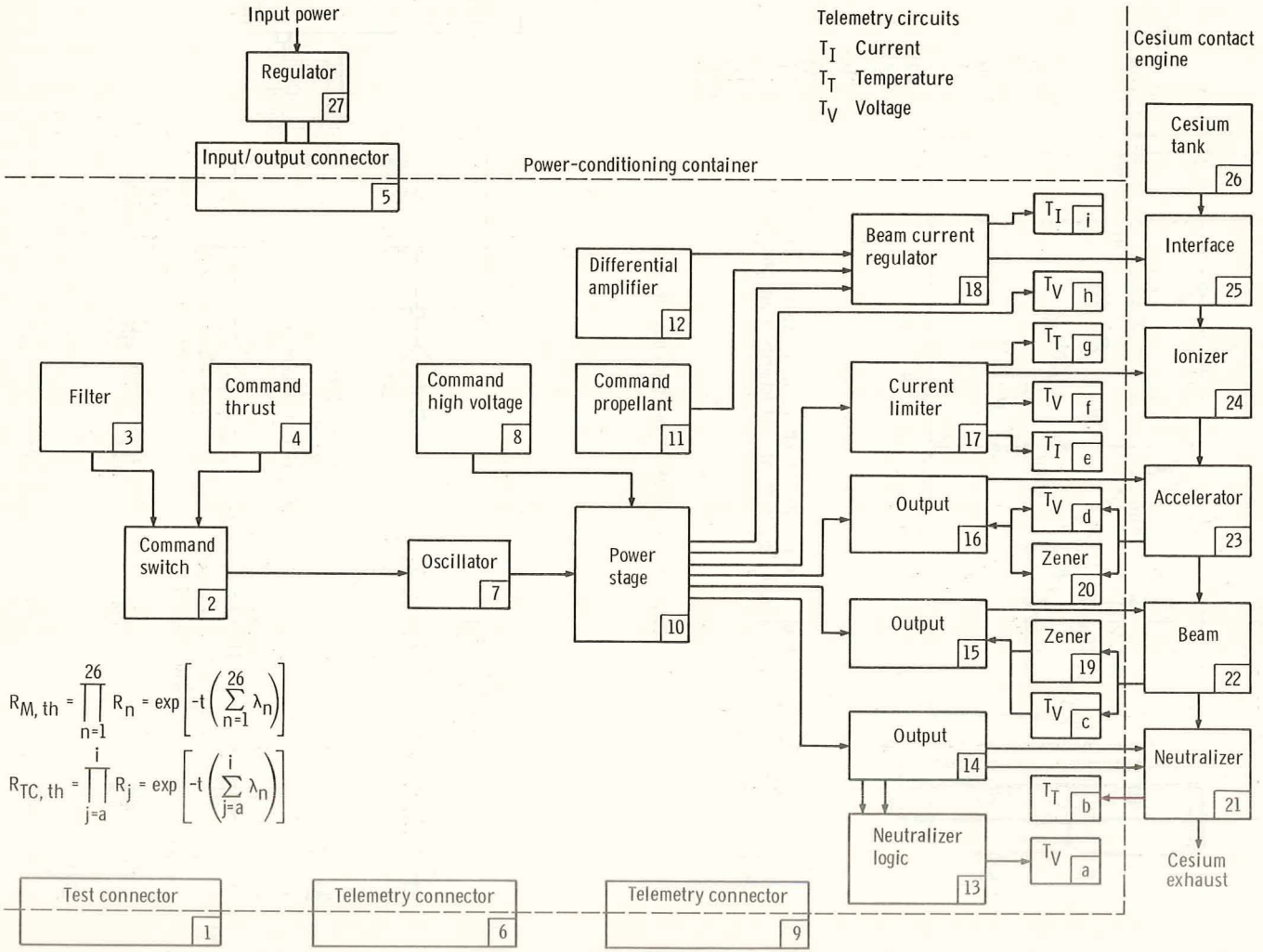

Figure 14. - Microthruster reliability model.

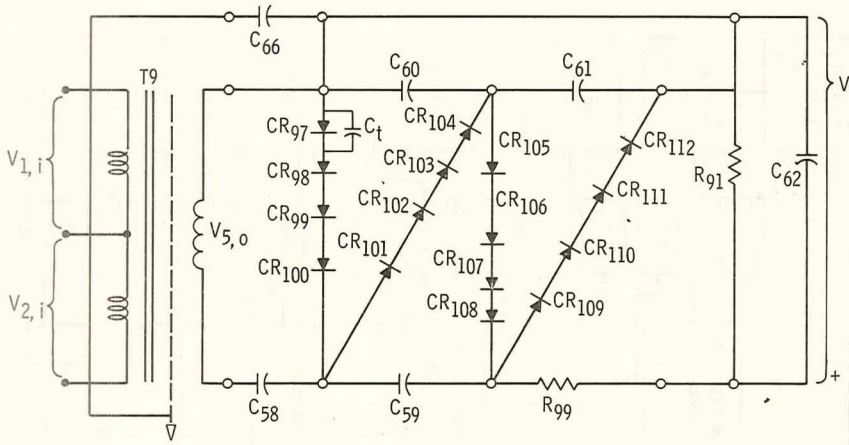

Schematic symbol	Added capacitance, (pF)
CR 97	27
98	0
99	54
100	156
101	156
102	30
103	0
104	45
105	24
106	0
107	45
108	150
109	72
110	0
111	5
112	60

Note:

1. Some specifications for this circuit are: Output voltage, 1.6 kilovolts dc; maximum output rectifier current, 3.0 milliamperes dc; frequency, 2 kilohertz; input potential, 24 volts dc; $\theta_{1,i} = -\theta_{2,i}$.

Figure 15. - Index 15 voltage quadrupler circuit.

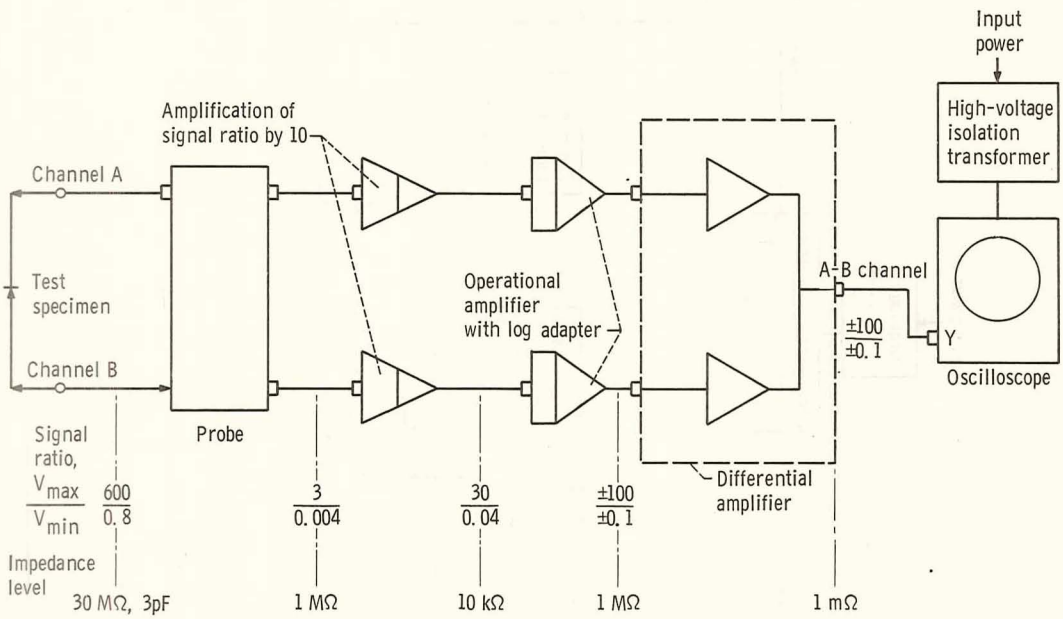

Figure 16. - Apparatus setup for rectifier voltage.

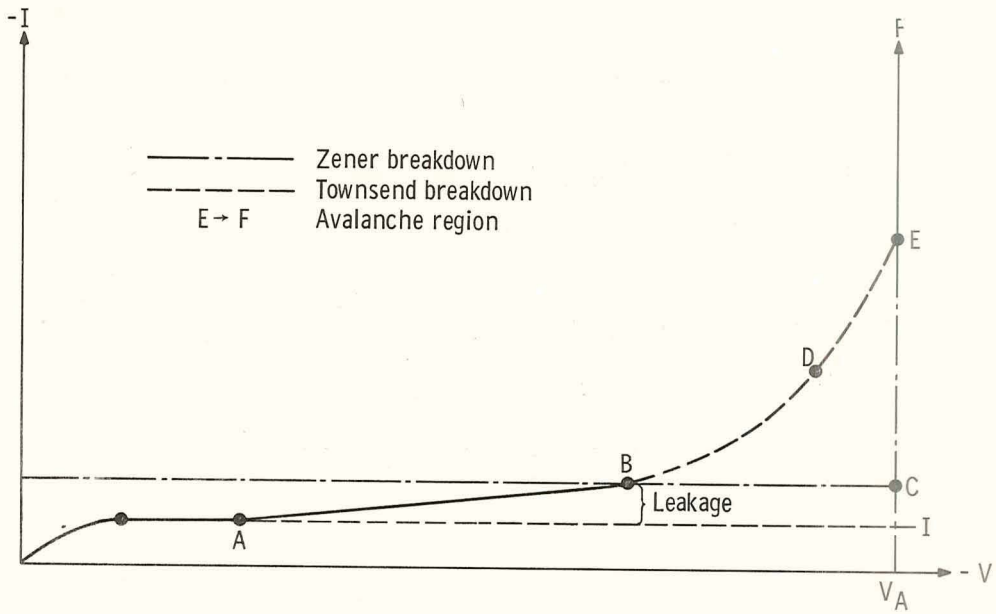

Figure 17. - Reverse voltage junction breakdown.

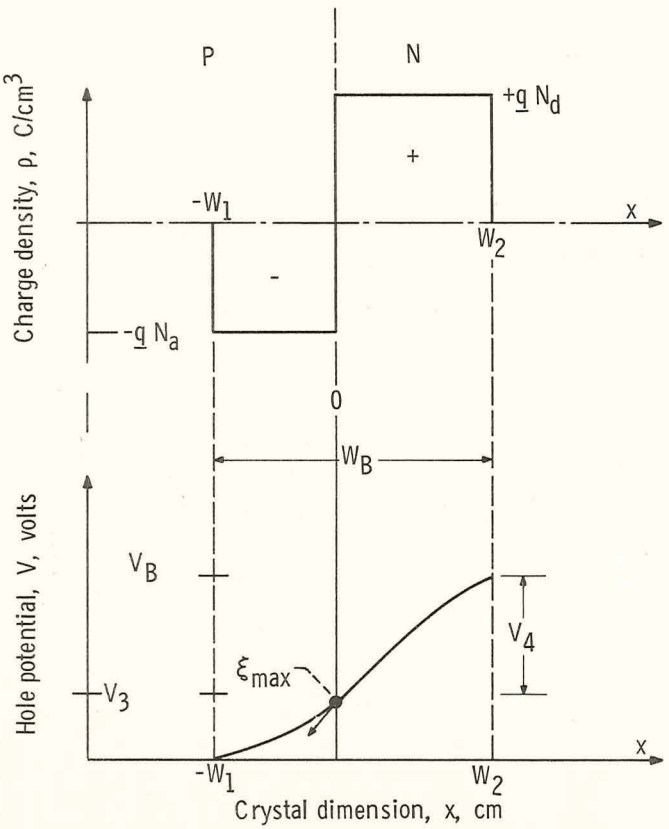

Figure 18. - Abrupt junction model.